NASA TN D-523

TECHNICAL NOTE
D-523

INVESTIGATION OF THE FLOW IN A RECTANGULAR CAVITY IN A FLAT PLATE AT A MACH NUMBER OF 3.55

By Russell W. McDearmon

Langley Research Center
Langley Field, Va.

NATIONAL AERONAUTICS AND SPACE ADMINISTRATION

WASHINGTON September 1960

NATIONAL AERONAUTICS AND SPACE ADMINISTRATION

TECHNICAL NOTE D-523

INVESTIGATION OF THE FLOW IN A RECTANGULAR CAVITY IN A FLAT PLATE AT A MACH NUMBER OF 3.55

By Russell W. McDearmon

SUMMARY

An investigation has been made in the Mach 3.5 blowdown jet of the Langley High-Temperature Fluid Mechanics Section of the flow in a rectangular cavity in a flat plate. The results indicate that a critical value of the ratio of depth to chord length existed between 0.093 and 0.146 such that the pressure distribution in the cavity was very sensitive to depth changes for ratios of depth to chord length less than the critical value and was insensitive to depth changes for ratios of depth to chord length greater than the critical value. Span variations had large effects on the pressure distribution only in the narrow cavities (cavities having ratios of span to chord length less than 0.25) at the moderately shallow depth (ratio of depth to chord length equal to 0.093). Varying the upstream and downstream lip radii caused large changes in the pressure distribution only in the moderately wide (ratio of span to chord length equal to 0.75), moderately shallow cavity.

The critical depth of the cavity and the pressure distribution in the very shallow cavity (ratio of depth to chord length equal to 0.042) were predicted analytically over the supersonic Mach number range, and the predictions agreed with experiment at a Mach number of 3.55.

The boundary layer of the flow approaching the cavity was turbulent.

INTRODUCTION

Designers of aircraft, missiles, and reentry vehicles encounter numerous problems which require knowledge of the flow characteristics in cavities. Among these problems is the estimation of the loads inside bomb bays and wells for purposes such as missile storage and retraction

of control surfaces and landing gear. Also, estimates of the drag contributions of these bomb bays and wells, and their effects on the other aerodynamic characteristics of the complete configurations, are needed. Furthermore, the discovery that the average heat transfer for separated boundary layers can be considerably less than that for equivalent attached boundary layers (see refs. 1 and 2) has created renewed interest in the flow phenomena in regions of separated flow, such as cavities.

Considerable research effort has been expended in seeking solutions to these problems. For example, references 3 and 4 present the results of wind-tunnel investigations at Mach numbers from 1.6 to 3.0 of the flow phenomena inside various bomb-bay configurations and the behavior of stores immediately following release. The effects of bomb-bay configuration upon the aerodynamic characteristics of bodies containing bomb bays were investigated at supersonic speeds in references 5 and 6. In reference 7 an attempt was made to determine the causes of the strong resonant oscillations which have occurred in cavities at supersonic speeds.

This report presents the results of an investigation at a Mach number of 3.55 of the effects of systematic variations of depth, span, and upstream and downstream lip radii on the flow characteristics in a rectangular cavity in a flat plate. The experimental phase of the investigation consisted of pressure-distribution measurements inside the cavity and schlieren photographs and shadowgraphs of the shock structure immediately above the cavity. The Reynolds number of the tests was 2.3×10^6, based on the distance from the leading edge of the flat plate to the upstream lip of the cavity, and the boundary layer of the flow approaching the cavity was turbulent. The critical depth (depth beyond which depth increases had no effect on the pressure distribution in the cavity) and the pressure distribution in the very shallow cavity were predicted analytically.

SYMBOLS

b	span of cavity
c	chord (streamwise) length of cavity
C_p	pressure coefficient, $\frac{p_l - p_\infty}{q_\infty}$
d	depth of cavity

l	length along bottom of cavity (fig. 11)
M	Mach number
p	static pressure
p_l	local pressure
p_t	total pressure
P	peak pressure-rise coefficient associated with separation of boundary layer
q_∞	free-stream dynamic pressure
r_u	radius of upstream cavity lip
r_d	radius of downstream cavity lip
U	velocity in free-stream direction
x	surface-contour distance measured in plane of symmetry of model; distances upstream of cavity lip are considered negative, and distances downstream of cavity lip are considered positive
y	perpendicular distance above top of plate
δ	thickness of boundary layer
ν	Prandtl-Meyer angle (angle through which a supersonic stream is turned to expand from $M = 1$ to $M > 1$)
φ	two-dimensional flow-deflection angle through shock

Subscripts:

0	conditions immediately upstream of cavity (fig. 11)
1	conditions in upstream corner of very shallow cavity (fig. 11)
2	conditions in midportion of very shallow cavity (fig. 11)
3	conditions in downstream corner of very shallow cavity (fig. 11)

4

4 conditions immediately downstream of cavity (fig. 11)

∞ free-stream conditions

APPARATUS

Wind Tunnel

The tests were conducted in the Mach 3.5 blowdown jet of the Langley High-Temperature Fluid Mechanics Section. For this facility, dry air from high-pressure storage tanks is exhausted through a stagnation chamber to a nozzle with a rectangular test section about 5 inches square. The air then passes through a fixed diffuser to the atmosphere. The pressure in the stagnation chamber can be controlled and held constant.

L
5
1
8

Models

A drawing of the model is presented in figure 1. The pressure distributions in the cavity were obtained by means of 0.020-inch-diameter orifices in the model and a multiple-tube mercury manometer. The locations of the orifices are given in figure 2. The various depths of the cavity and the provisions for varying the upstream and downstream lip radii are also shown in figure 2.

The cavity was located in the plate so that the Mach lines from the corners of the leading edge fell outside of the cavity side faces. The model was made of steel and the top of the plate and the interior surfaces of the cavity were highly polished. The leading edge of the plate was made as sharp as possible. The depth and chord length of the cavities were varied by means of metal inserts, and the span and lip-radii variations were obtained by using mahogany inserts. Any gaps in the exposed surfaces resulting from the insertions were carefully filled in with plaster.

All model configurations were tested with and without an aluminum-oxide transition strip on the plate (abbreviated "t.s." on the figures). The strip was approximately 0.007 inch thick; other dimensions and the locations of the strip are given in figure 1.

PRECISION

The estimated probable errors in the test parameters and variables are as follows:

M	±0.05
C_p:	
For $\lvert C_p \rvert = 0.010$	±0.0004
For $\lvert C_p \rvert = 0.200$	±0.008
For $\lvert C_p \rvert = 1.300$	±0.030
x/c	±0.002
d/c	±0.001
b/c	±0.01
r_u/c	±0.01
r_d/c	±0.01

The angle of attack of the top of the flat plate was maintained at 0°, within $+0.1^\circ$ and -0.0°.

Throughout the tests the moisture content in the tunnel was ascertained (by dewpoint measurements) to be so low that the effects of condensation were negligible.

RESULTS AND DISCUSSION

Boundary Layer

In order to identify the boundary layer of the flow approaching the cavity, pitot surveys were made immediately ahead of the upstream cavity lip. (The exact location of the survey was 97 percent of the distance from the plate leading edge to the upstream cavity lip on the longitudinal center line of the plate.) Surveys were made with and without a transition strip affixed near the plate leading edge.

The boundary-layer Mach number distributions obtained in the surveys are presented in figure 3(a). The presence of the transition strip had little effect on the shape of the curve, although it increased the boundary-layer thickness from approximately 0.043 inch to 0.054 inch.

Nondimensional velocity profiles were computed and are compared with theoretical laminar profiles from reference 8 and theoretical turbulent profiles in figure 3(b). The experimental profiles with the transition strip off and on agree well with the 1/9-power turbulent profile; this indicates that natural transition from laminar to turbulent flow occurred on the plate upstream of the cavity.

Pressure-distribution measurements in the cavity with the transition strip off and on were made over the range of depth, span, and

lip-radii variations of the tests. The transition strip had negligible effects on the pressure distributions; therefore the data with the transition strip on will not be presented.

Effects of Depth on Flow in Cavity

Pressure distributions.- The effects of depth on the pressure distribution in the cavity are shown in figure 4. The data presented were obtained for the widest cavity tested for each chord length ($b/c = 2.00$ for $c = 0.500$ inch and $c = 1.000$ inch; $b/c = 1.25$ for $c = 1.500$ inches) so that the influence of the cavity side faces on the data was minimized.

Figure 4 shows that markedly different pressure distributions were obtained for $d/c = 0.042$ and $d/c = 0.093$. Increasing d/c from 0.093 to 0.146 further changed the pressure distribution, whereas nearly the same distributions were obtained on the upstream face and bottom for $d/c = 0.202$, 0.329, and 0.457 as for $d/c = 0.146$. This indicated that a critical value of d/c existed between 0.093 and 0.146 (hereinafter referred to as $(d/c)_{critical}$) such that the pressure distribution was very sensitive to depth changes for $d/c < (d/c)_{critical}$ and was insensitive to depth changes for $d/c > (d/c)_{critical}$.

Figure 4 also shows that for the wide cavities d/c was a sufficient parameter for defining the pressure distribution; that is, the pressure distribution was independent of c at all depths except for small effects of c in the downstream corner.

Schlieren photographs and shadowgraphs.- Figure 5 presents schlieren photographs and shadowgraphs of the shock structure immediately above the wide cavities over the range of depths for which pressure distributions were measured. Study of the schlieren photographs and shadowgraphs and the corresponding pressure distributions of figure 4 indicates that the flow phenomena in the cavities were as shown in the following sketches:

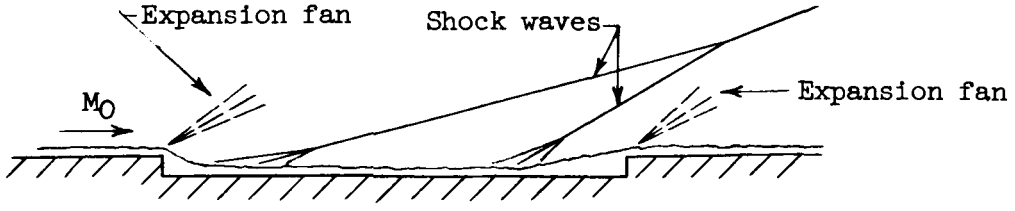

Sketch (a) $d/c = 0.042$; $b/c = 1.25$ and 2.00.

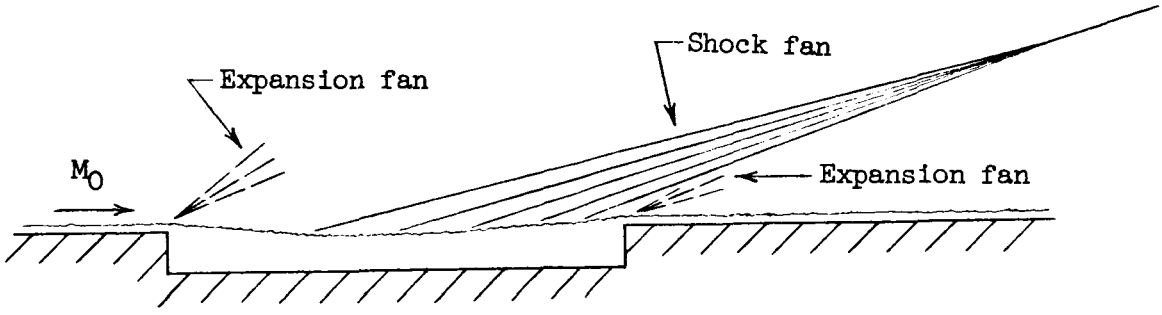

Sketch (b) $d/c = 0.093$; $b/c = 1.25$ and 2.00.

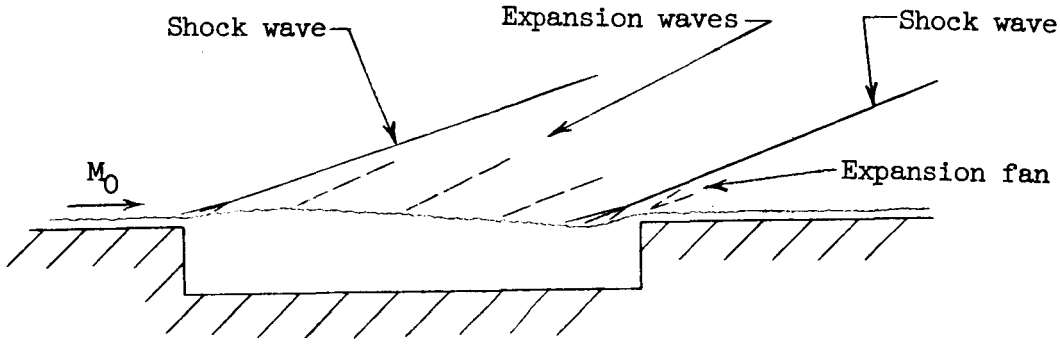

Sketch (c) $d/c = 0.146$; $b/c = 1.25$ and 2.00.

Figure 4(a) shows that for $d/c = 0.042$ the flow became attached to the cavity bottom, as depicted in sketch (a); that is, a large pressure decrease was obtained in the upstream corner followed by recovery to free-stream pressure. Figure 4(b) shows that for $d/c = 0.093$ the flow was detached from the bottom, as depicted in sketch (b), since the amount the flow could turn, commensurate with the decrease in pressure obtained in the upstream corner, was insufficient for the flow to become attached to the bottom. These facts indicate that a value of d/c existed between 0.042 and 0.093 at which the flow just became detached from the bottom; this value will be designated $(d/c)_{detached}$. Figures 4(c) to 4(f) show that for $d/c = 0.146$, 0.202, 0.329, and 0.457 the flow was also detached from the bottom, as depicted for $d/c = 0.146$ in sketch (c), although the flow phenomena were different from those for $d/c = 0.093$. (See sketch (b).)

In conclusion, d/c not only influenced the pressure distribution for depths sufficiently small for the flow to be attached to the cavity

bottom $\left(d/c < (d/c)_{detached}\right)$, but continued to affect the pressure distribution beyond the depth $(d/c = 0.093)$ for which the flow was completely separated from the bottom. Only when the depth reached $(d/c)_{critical}$, a value of d/c between 0.093 and 0.146, did the flow assume a "constant" character which was unaltered by further depth increases.

Effects of Span on Flow in Cavity

Pressure distributions.- The effects of span variations on the pressure distribution in the cavity are presented in figure 6. This figure shows that the pressure distribution was very sensitive to span variations only for the narrow cavities of moderately shallow depth $(d/c = 0.093)$. At this depth nearly identical pressure distributions were obtained for $b/c = 0.13$ and 0.19. (See fig. 6(a).) These pressure distributions consisted of sizable decreases in pressure below p_∞ in the upstream corner and very large increases in pressure above p_∞ in the downstream corner. Increasing the span from $b/c = 0.19$ to 0.25 caused the pressure to rise in the upstream corner and fall drastically in the downstream corner. Further increases in the span (from $b/c = 0.25$ to 2.00) affected the pressure distributions only slightly.

For the very shallow cavity $(d/c = 0.042)$ increasing the span from $b/c = 0.13$ to 0.38 altered the pressure distribution in the downstream corner in a systematic manner. (See fig. 6(a).) Further increases in b/c (from 0.38 to 2.00) did not change the basic shape of the pressure-distribution curves throughout the entire cavity (fig. 6(b)).

For the deep cavities $(d/c \geq 0.146)$ increasing b/c from 0.13 to 2.00 did not appreciably affect the pressure distributions.

Care should be exercised in any application of the results for $d/c = 0.093$, such as determination of the drag contribution of the downstream face, because the downstream face of this cavity contained only one orifice and the fairings in the vicinity of the downstream face are therefore uncertain.

Schlieren photographs.- Figure 7 presents schlieren photographs showing the effects of span variations on the shock structure immediately above the moderately shallow cavity $(d/c = 0.093)$. Study of the photographs for $b/c = 0.13$ and 0.19 and the corresponding pressure distributions of figure 6(a) indicates that the flow phenomena in the very narrow cavities were as shown in the following sketch:

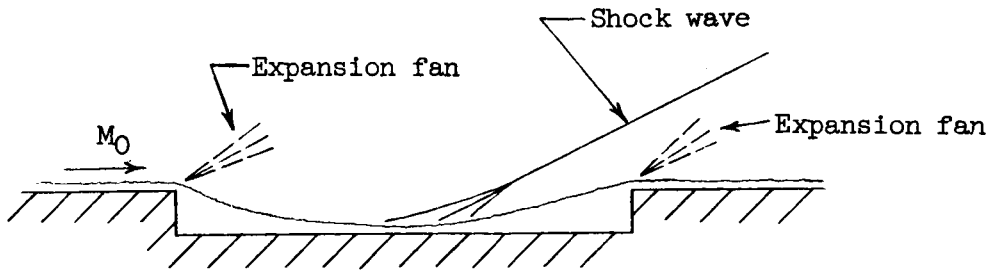

Sketch (d) $d/c = 0.093$; $b/c = 0.13$ or 0.19.

The flow turned downward into the cavity at approximately the same angle as shown for the very wide ($b/c = 2.00$), very shallow cavity ($d/c = 0.042$) in sketch (a) of a preceding section, but the flow apparently did not become attached to the bottom, as occurred for $d/c = 0.042$. Increasing b/c to 0.25 caused the flow phenomena to revert to that shown in sketch (b) of a preceding section.

Effects of Spanwise Location on Pressure Distribution in Cavity

Figure 8 presents the effects of spanwise location on the longitudinal pressure distribution in a moderately wide cavity ($b/c = 0.75$). Nearly identical pressure distributions were obtained in the center and near the side for the shallow and deep versions of this cavity, indicating that the spanwise location of the pressure measurements had no effect on the pressure distribution in a moderately wide cavity.

Effects of Upstream and Downstream Lip Radii on Flow in Cavity

Pressure distributions.- The effects of upstream and downstream lip radii on the pressure distribution in the cavity are presented in figure 9. Figure 9(a) shows that for the moderately wide version ($b/c = 0.75$) of the moderately shallow cavity ($d/c = 0.093$), changing both r_u/c and r_d/c from 0 to 0.08 markedly changed the pressure distribution, whereas either changing r_u/c or r_d/c from 0 to 0.08 while the other remained 0, or changing both r_u/c and r_d/c from 0 to 0.03, did not affect the pressure distribution. Figure 9(a) also shows that the pressure distributions in the deep versions of the moderately wide cavity were unaffected by the variations in lip radii.

For the very narrow ($b/c = 0.13$), moderately shallow cavity ($d/c = 0.093$), figure 9(b) shows a general trend toward slightly

reduced pressures in the downstream corner when the downstream lip was rounded.

For the very wide ($b/c = 2.00$), moderately shallow cavity ($d/c = 0.093$), figure 9(c) shows that the pressure distribution was unaffected by variations in lip radii.

Schlieren photographs and shadowgraphs.- Figure 10 presents schlieren photographs showing the effects of upstream and downstream lip radii on the shock structure immediately above the moderately wide ($b/c = 0.75$), moderately shallow cavity ($d/c = 0.093$). Study of the photographs and the corresponding pressure distributions of figure 9(a) indicates that changing both r_u/c and r_d/c from 0 to 0.08 caused changes in the flow phenomena which were quite similar to those obtained in the square-lipped cavities having $d/c = 0.093$ when the span was reduced from $b/c = 0.25$ to 0.19. (See the preceding section entitled "Effects of Span on Flow in Cavity.") The flow phenomena in the moderately shallow cavity were very sensitive to configuration changes, since either of the above changes caused the flow to change from dipping slightly into the cavity to dipping deeply into the cavity and probably striking the bottom. Thus the value of d/c for which the flow just became detached from the bottom of the very wide cavity ($b/c = 2.00$) may have been close to 0.093.

L 5 1 8

Prediction of Critical Depth of Cavity

An attempt has been made to predict the critical depth of the cavity over the supersonic Mach number range. This attempt consisted of determining $(d/c)_{detached}$ for the cavity by analyzing a simplified version of supersonic flow in a very shallow two-dimensional cavity and then studying the changes in the flow pattern which occurred as the depth was increased to $(d/c)_{detached}$. Figure 11 presents a sketch of the simplified version of the flow. The boundary layer was neglected and the flow was assumed to turn abruptly upon attaching to and separating from the cavity bottom, whereas more gradual turning of the flow occurred in actuality, such as was depicted in sketch (a). Thus the predicted $(d/c)_{detached}$ would be expected to exceed the actual $(d/c)_{detached}$. Experimentally, $(d/c)_{critical}$ was larger than $(d/c)_{detached}$ (see preceding section entitled "Effects of Depth on Flow in Cavity"), and therefore the predicted $(d/c)_{detached}$ should provide a fair estimate of $(d/c)_{critical}$. The details of the method of predicting $(d/c)_{detached}$ are presented in a subsequent section of this report.

The predicted variation of $(d/c)_{detached}$ with M_0 and comparison with the experimental results at $M_0 = 3.55$ are presented in figure 12.

The predicted $(d/c)_{detached}$ falls between the limits of experimental $(d/c)_{critical}$ at $M_0 = 3.55$.

Comparison of Experimental Pressure Distribution in Very Shallow Cavity With Predicted Pressure Distribution

The experimental pressure distribution in the very shallow cavity $(d/c) = 0.042$) is compared with a predicted pressure distribution in figure 13. The method of predicting the pressure distribution is explained in a subsequent section of this report; the simplified version of the flow which was used in predicting $(d/c)_{detached}$ is also used in predicting the pressure distribution. Figure 13 shows that the predicted pressure distribution agreed well with experiment on the upstream and downstream faces, but that pressure gradients existed along the bottom rather than the finite pressure discontinuities which resulted from using the simplified nonviscous version of the flow.

L 5 1 8

ANALYTICAL METHODS

Prediction of Detachment Depth of Cavity

Referring to the sketch of figure 11, $(d/c)_{detached}$ is the value of d/c for the case in which the bottom has been lowered until l_2 vanishes. For a very shallow cavity $(i.e., \ d/c < (d/c)_{detached})$,

$$c = l_1 + l_2 + l_3 = d \cot \varphi_2 + l_2 + d \cot \varphi_3$$

or

$$\frac{d}{c} = \frac{1 - \frac{l_2}{c}}{\cot \varphi_2 + \cot \varphi_3}$$

Increasing the depth to the detachment depth $(i.e.,$ setting l_2 equal to $0)$ gives

$$\left(\frac{d}{c}\right)_{detached} = \frac{1}{\cot \varphi_2 + \cot \varphi_3} \qquad (1)$$

The values of φ_2 and φ_3 will now be determined for $d/c < (d/c)_{detached}$ (i.e., l_2 small but unequal to zero) and will be assumed to hold for $d/c = (d/c)_{detached}$.

Consider region 1 to be the area behind a rearward-facing step. Assume that the flow phenomena behind a rearward-facing step are analogous to those ahead of a forward-facing step. Reference 9 established the analogy between the flow phenomena for a two-dimensional base and a forward-facing step. Hence the only new assumption being made in the present analysis is that replacing the horizontal center plane of the base of reference 9 with a flat surface does not alter the flow behind the base.

The peak pressure-rise coefficient associated with the separation of a turbulent boundary layer ahead of a forward-facing step throughout the supersonic Mach number range (Mach numbers between 1 and 4) was defined in reference 10 by the empirical relation

$$P = \frac{3.2}{8 + (M_\infty - 1)^2} \tag{2}$$

This relation may not account for all the possible effects on P of Reynolds number, boundary-layer thickness, and step height, such as are presented in reference 11. However, reference 11 shows that equation (2) gave a good mean evaluation of P over the supersonic Mach number range, particularly in the Reynolds number range of the present tests.

Application of the analogy between the flow phenomena for rearward-facing and forward-facing steps to regions 1 and 2 of figure 11 gives $P = \frac{p_2 - p_1}{q_1} = \frac{3.2}{8 + (M_1 - 1)^2}$. Thus the static-pressure ratio across the oblique shock wave attending separation from the cavity bottom is

$$\frac{p_2}{p_1} = 0.7M_1^2 \frac{3.2}{8 + (M_1 - 1)^2} + 1.0 \tag{3}$$

The two-dimensional flow-deflection angle through the shock is given by

$$\varphi_2 = \tan^{-1}\left\{\frac{5\left(\frac{p_2}{p_1} - 1\right)}{7M_1^2 - 5\left(\frac{p_2}{p_1} - 1\right)}\left[\frac{7M_1^2 - \left(6\frac{p_2}{p_1} + 1\right)}{6\frac{p_2}{p_1} + 1}\right]^{1/2}\right\} \tag{4}$$

Substitution of equation (3) into equation (4) gives

$$\varphi_2 = \tan^{-1}\left[2.667M_1^2\left(\frac{M_1^4 - 2M_1^3 + 6.08M_1^2 + 2M_1 - 9}{2.92M_1^2 - 2M_1 + 9}\right)^{1/2}\right] \tag{5}$$

In the present tests the boundary layer of the flow approaching the cavity was turbulent (see preceding section entitled "Boundary Layer"); therefore equation (5) may be used to compute φ_2 for supersonic values of M_1. A supersonic range of M_0 corresponding to the values of M_1 is determined by assuming a Prandtl-Meyer expansion around the upstream lip $(\nu_0 = \nu_1 - \varphi_2)$.

Consider region 3 to be the area ahead of a forward-facing step. Then

$$\varphi_3 = \tan^{-1}\left[2.667M_2^2\left(\frac{M_2^4 - 2M_2^3 + 6.08M_2^2 + 2M_2 - 9}{2.92M_2^2 - 2M_2 + 9}\right)^{1/2}\right] \tag{6}$$

Values of M_2 corresponding to the supersonic range of M_0 are obtained from reference 12 by considering M_2 to be the flow over a wedge having a semivertex angle φ_2. Thus φ_3 can be computed from equation (6), and $(d/c)_{detached}$ can now be evaluated by using equation (1).

Prediction of Pressure Distribution in Very Shallow Cavity

The pressure distribution in a very shallow two-dimensional cavity $\left(d/c < (d/c)_{detached}\right)$ at supersonic speeds may be determined in the following manner (see fig. 11):

Region 1.- Assume that the flow expands isentropically around the upstream lip and therefore $p_{t,0} = p_{t,1}$. The value of p_1 is readily found by using a measured value of $p_{t,0}$ for $p_{t,1}$ and the value of p/p_t from reference 12 for the value of M_1 which corresponds to the value of M_0 under consideration.

Region 2.- The value of p_2 is found by using equation (3).

Region 3.- For application to regions 2 and 3, equation (3) becomes

$$\frac{p_3}{p_2} = 0.7M_2^2 \frac{3.2}{8 + (M_2 - 1)^2} + 1.0 \qquad (7)$$

Compute p_3 by using equation (7) and the value of M_2 which corresponds to the value of M_0 under consideration. (See previous section, "Prediction of Detachment Depth of Cavity.")

Region 4.- Compute $p_{t,4}$ by determining the successive losses in $p_{t,0}$ which result from the presence of the two shock waves inside the cavity. The value of p_4 is found by using this value of $p_{t,4}$ and the value of p/p_t from reference 12 for the value of M_4 which corresponds to the value of M_0 under consideration. The value of M_4 is determined by assuming a Prandtl-Meyer expansion around the downstream lip $(\nu_4 = \nu_3 + \varphi_3)$.

CONCLUSIONS

The results of an investigation of the flow in a rectangular cavity in a flat plate at a Mach number of 3.55 and a Reynolds number of 2.3×10^6 indicate the following conclusions:

1. A critical value of the ratio of depth to chord length d/c existed between 0.093 and 0.146 such that the pressure distribution in the cavity was very sensitive to depth changes for d/c less than $(d/c)_{critical}$, and was insensitive to depth changes for d/c greater than $(d/c)_{critical}$.

2. Variations in the span b had large effects on the pressure distribution only in the narrow cavities ($b/c < 0.25$) at the moderately shallow depth ($d/c = 0.093$).

3. Varying the upstream and downstream lip radii caused large changes in the pressure distribution only in the moderately wide ($b/c = 0.75$), moderately shallow cavity ($d/c = 0.093$).

4. The critical depth of the cavity and the pressure distribution in the very shallow cavity ($d/c = 0.042$) were predicted analytically over the supersonic Mach number range, and the predictions agreed with experiment at Mach 3.55. The pressures in the deep cavities ($d/c \geq 0.146$) were essentially equal to the stream static pressure, except in the downstream corner.

Langley Research Center,
National Aeronautics and Space Administration,
Langley Field, Va., March 1, 1960.

REFERENCES

1. Chapman, Dean R.: A Theoretical Analysis of Heat Transfer in Regions of Separated Flow. NACA TN 3792, 1956.

2. Larson, Howard K.: Heat Transfer in Separated Flows. Rep. No. 59-37, Inst. Aero. Sci., Jan. 1959.

3. Kamrass, Murray: Supersonic Wind Tunnel Investigation of Flow in Various Bomb Bay Configurations. Rep. No. GC-910-C-19 (Contract AF 33(616)-2394), Cornell Aero. Lab., Inc., Sept. 1957.

4. Rainey, Robert W.: A Wind-Tunnel Investigation of Bomb Release at a Mach Number of 1.62. NACA RM L53L29, 1954.

5. Rainey, Robert W.: Investigation of the Effects of Bomb-Bay Configuration Upon the Aerodynamic Characteristics of a Body With Circular Cross Section at Supersonic Speeds. NACA RM L55E27, 1955.

6. Rainey, Robert W.: Investigation at Supersonic Speeds of the Effects of Bomb-Bay Configuration Upon the Aerodynamic Characteristics of Fuselages With Noncircular Cross Sections. NACA RM L56H20, 1956.

7. Gibson, John Edward, Jr.: An Analysis of Supersonic Cavity Flow. Tech. Rep. 299 (Contracts Nonr 1841(40) and AF 33(616)-3909, Naval Supersonic Lab., M.I.T., May 1958.

8. Chapman, Dean R., and Rubesin, Morris W.: Temperature and Velocity Profiles in the Compressible Laminar Boundary Layer With Arbitrary Distribution of Surface Temperature. Jour. Aero. Sci., vol. 16, no. 9, Sept. 1949, pp. 547-565.

9. Love, Eugene S.: Base Pressure at Supersonic Speeds on Two-Dimensional Airfoils and on Bodies of Revolution With and Without Fins Having Turbulent Boundary Layers. NACA TN 3819, 1957. (Supersedes NACA RM L53C02.)

10. Love, Eugene S.: Pressure Rise Associated With Shock-Induced Boundary-Layer Separation. NACA TN 3601, 1955.

11. Chapman, Dean R., Kuehn, Donald M., and Larson, Howard K.: Investigation of Separated Flows in Supersonic and Subsonic Streams with Emphasis on the Effect of Transition. NACA Rep. 1356, 1958. (Supersedes NACA TN 3869.)

12. Ames Research Staff: Equations, Tables, and Charts for Compressible Flow. NACA Rep. 1135, 1953. (Supersedes NACA TN 1428.)

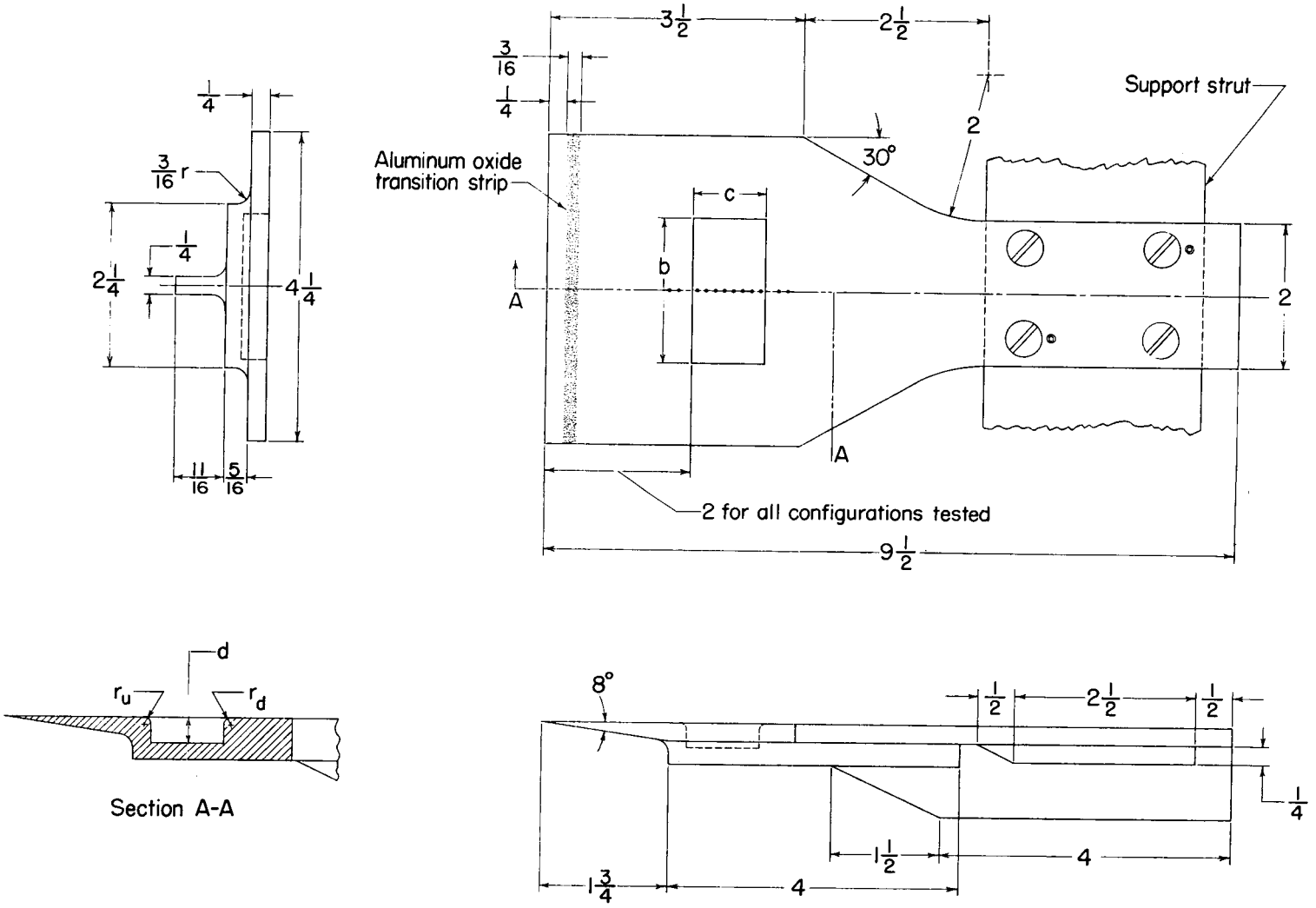

Figure 1.- Drawing of model. All dimensions are in inches.

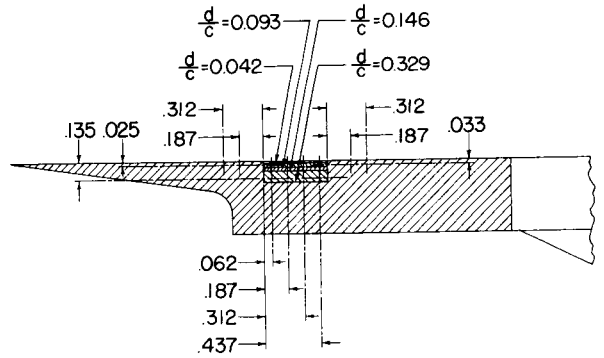

Section A-A, c=0.500 in. (square lips)

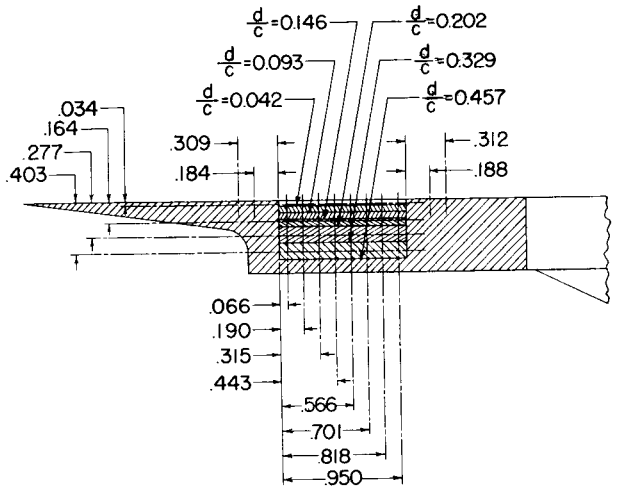

Section A-A, c=1.000 in. (square lips)

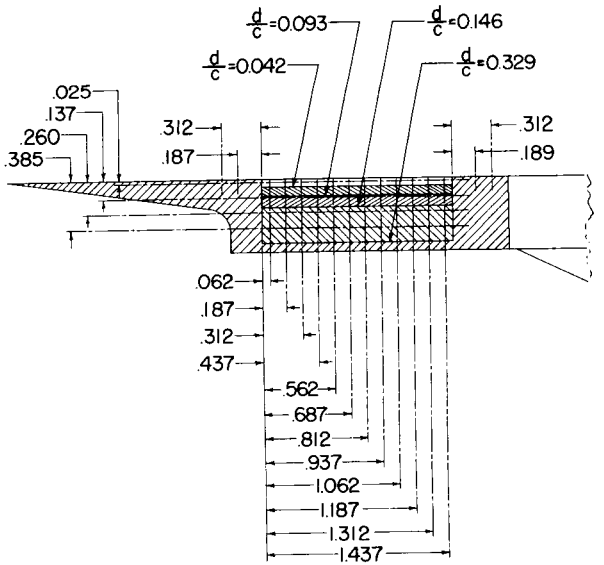

Section A-A, c=1.500 in. (square lips)

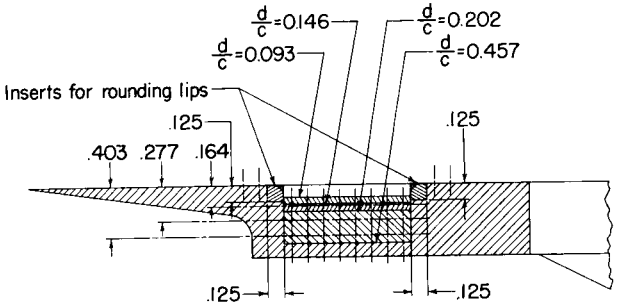

Note: Orifice locations on bottom of cavity and top of plate are same as for c=1.000 in., square lips.

Section A-A, c=1.000 in. (round lips)

Figure 2.- Location of orifices in model. All dimensions are in inches.

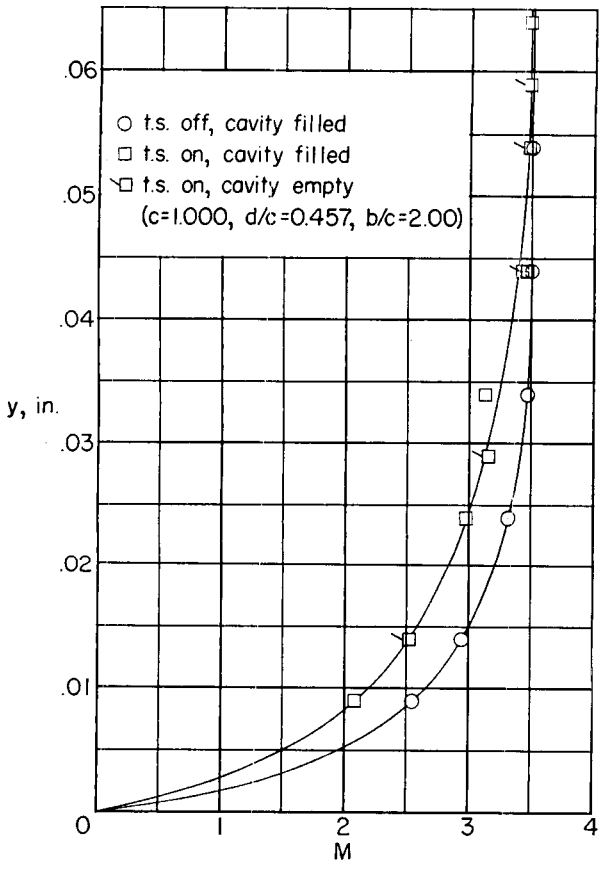

(a) Mach number distributions with and without transition strip near the plate leading edge.

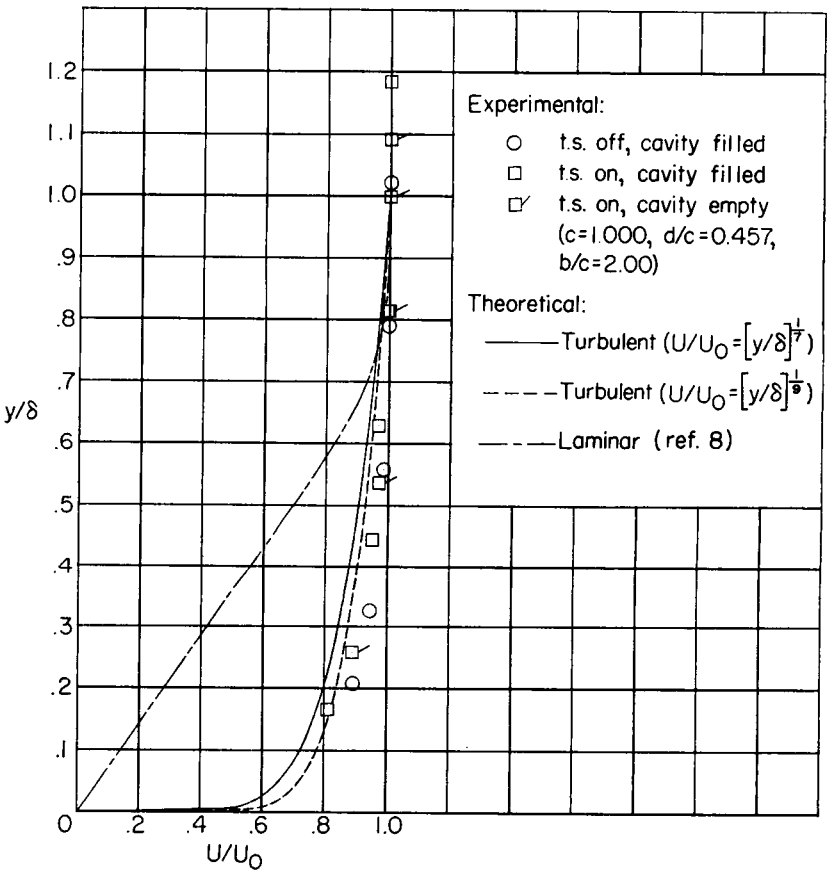

(b) Comparison of nondimensional velocity profiles with theoretical laminar and turbulent profiles.

Figure 3.- Results of pitot survey of plate boundary layer immediately ahead of upstream lip of cavity.

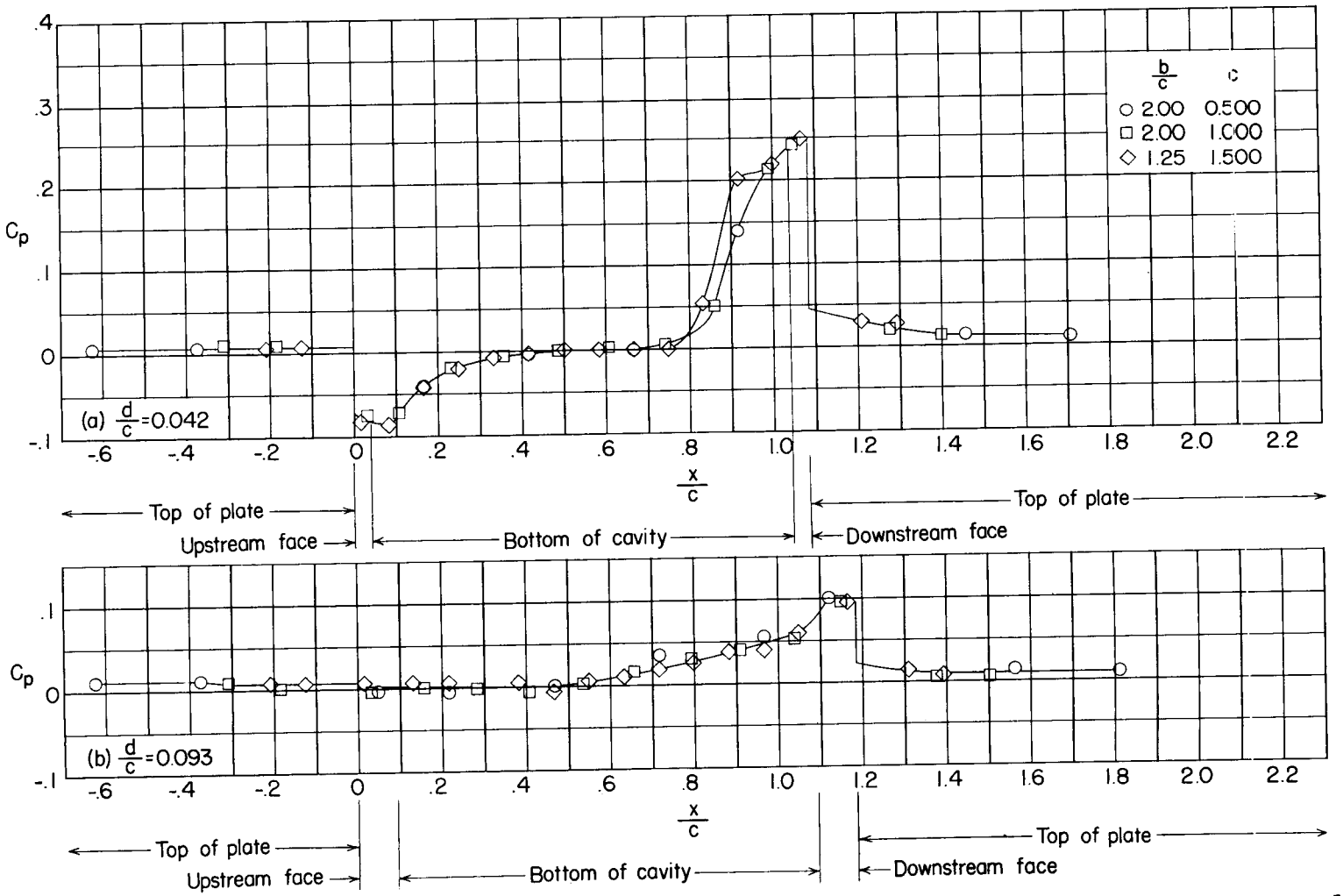

Figure 4.- Effect of depth on the pressure distribution in the cavity. (Dashed portions of curves indicate uncertain fairing.)

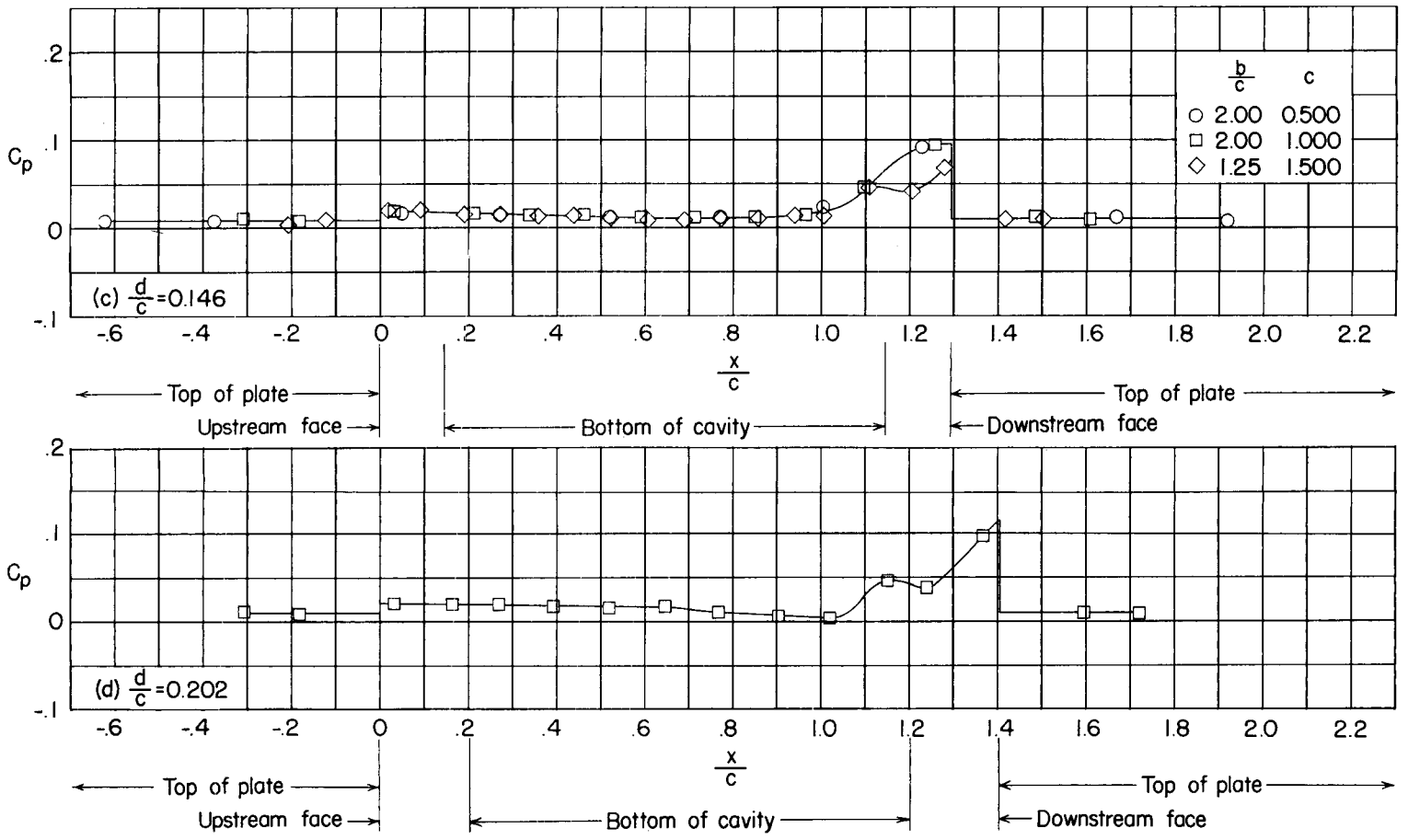

Figure 4.- Continued.

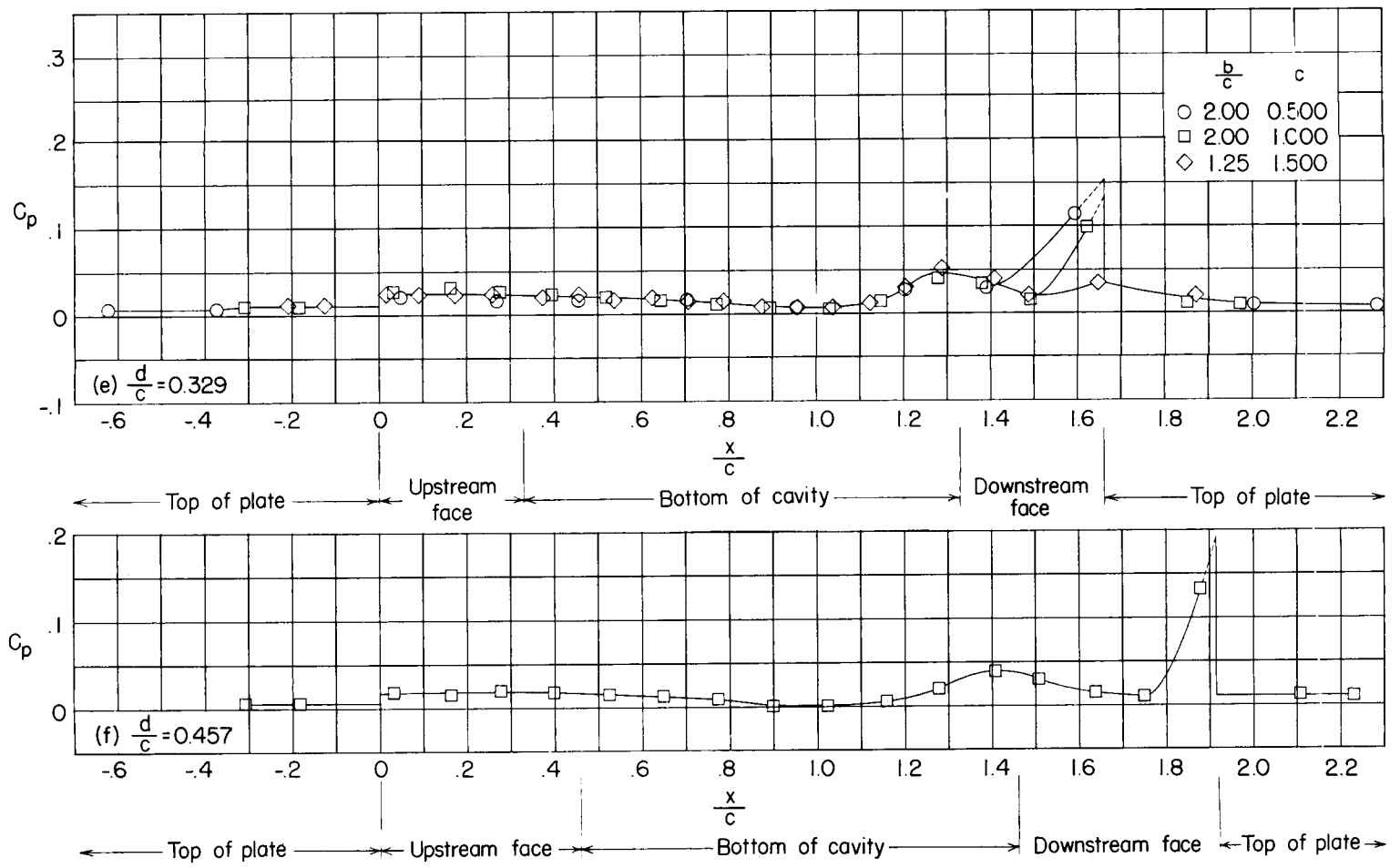

Figure 4.- Concluded.

$\frac{d}{c}$=0.042, $\frac{b}{c}$=2.00, t.s. off

$\frac{d}{c}$=0.093, $\frac{b}{c}$=2.00, t.s. on

SCHLIERENS

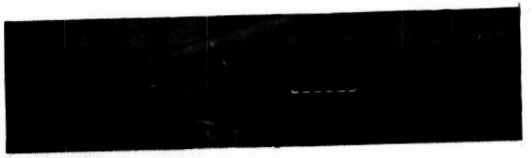

$\frac{d}{c}$=0.042, $\frac{b}{c}$=2.00, t.s. off

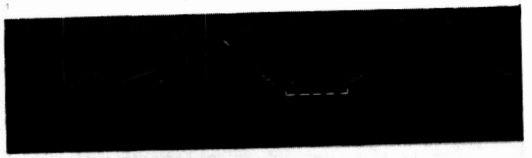

$\frac{d}{c}$=0.093, $\frac{b}{c}$=2.00, t.s. on

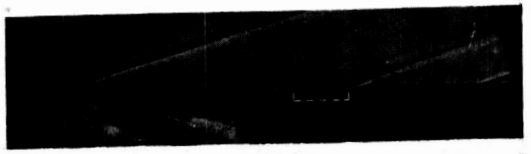

$\frac{d}{c}$=0.146, $\frac{b}{c}$=2.00, t.s. off

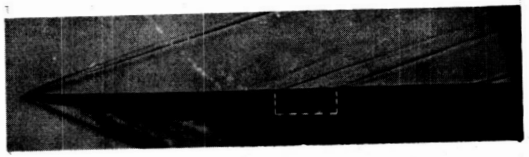

$\frac{d}{c}$=0.329, $\frac{b}{c}$=2.00, t.s. off

SHADOWGRAPHS

(a) c = 0.500 inch. L-60-266

Figure 5.- Photographs showing the effects of depth on the shock structure immediately above the cavities.

$\frac{d}{c}$=0.042, $\frac{b}{c}$=2.00, t.s. on

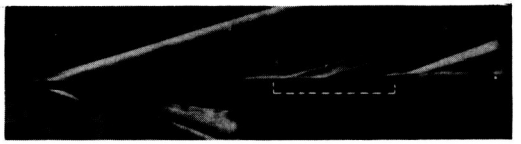

$\frac{d}{c}$=0.093, $\frac{b}{c}$=2.00, t.s. off

$\frac{d}{c}$=0.146, $\frac{b}{c}$=2.00, t.s. off

$\frac{d}{c}$=0.457, $\frac{b}{c}$=0.38, t.s. on

SCHLIERENS

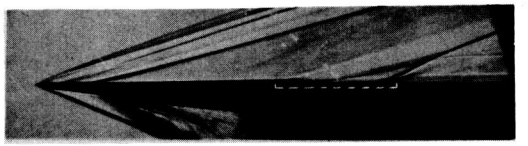

$\frac{d}{c}$=0.042, $\frac{b}{c}$=2.00, t.s. on

$\frac{d}{c}$=0.093, $\frac{b}{c}$=2.00, t.s. off

$\frac{d}{c}$=0.146, $\frac{b}{c}$=2.00, t.s. off

$\frac{d}{c}$=0.457, $\frac{b}{c}$=0.75, t.s. on

SHADOWGRAPHS

(b) c = 1.000 inch. L-60-267

Figure 5.- Continued.

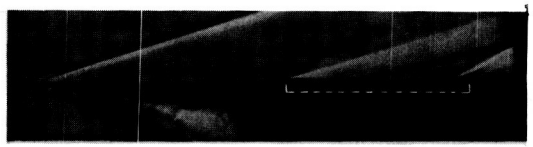

$\frac{d}{c}$=0.042, $\frac{b}{c}$=1.25, t.s. off

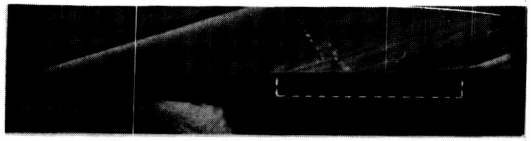

$\frac{d}{c}$=0.093, $\frac{b}{c}$=1.25, t.s. off

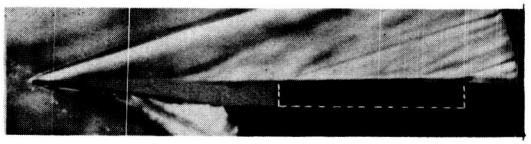

$\frac{d}{c}$=0.146, $\frac{b}{c}$=1.25, t.s. off

$\frac{d}{c}$=0.329, $\frac{b}{c}$=1.25, t.s. off

SCHLIEREN

$\frac{d}{c}$=0.042, $\frac{b}{c}$=1.25, t.s. off

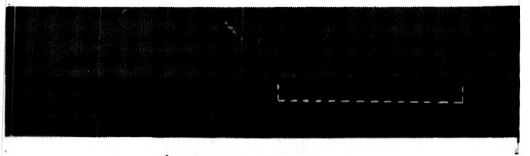

$\frac{d}{c}$=0.093, $\frac{b}{c}$=1.25, t.s. off

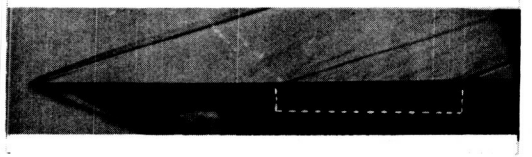

$\frac{d}{c}$=0.146, $\frac{b}{c}$=1.25, t.s. off

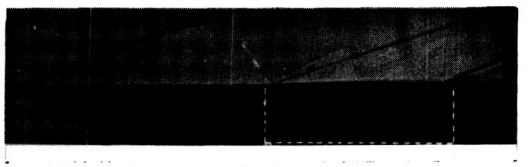

$\frac{d}{c}$=0.329, $\frac{b}{c}$=1.25, t.s off

SHADOWGRAPHS

(c) c = 1.500 inches.

L-60-268

Figure 5.- Concluded.

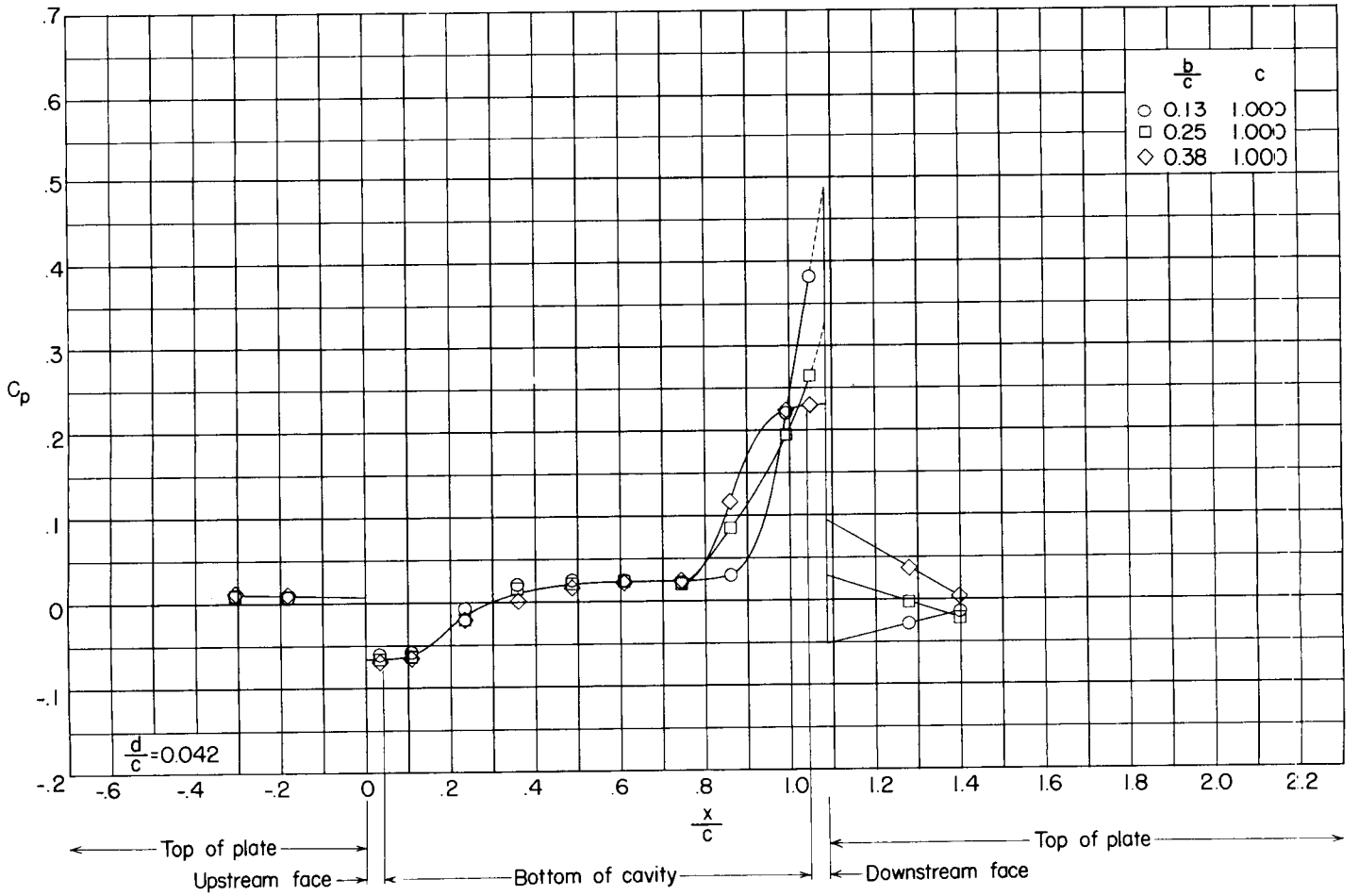

(a) $\frac{b}{c}$ = 0.13 to 0.38.

Figure 6.- Effect of span on the pressure distribution in the cavity. (Dashed portions of curves indicate uncertain fairing.)

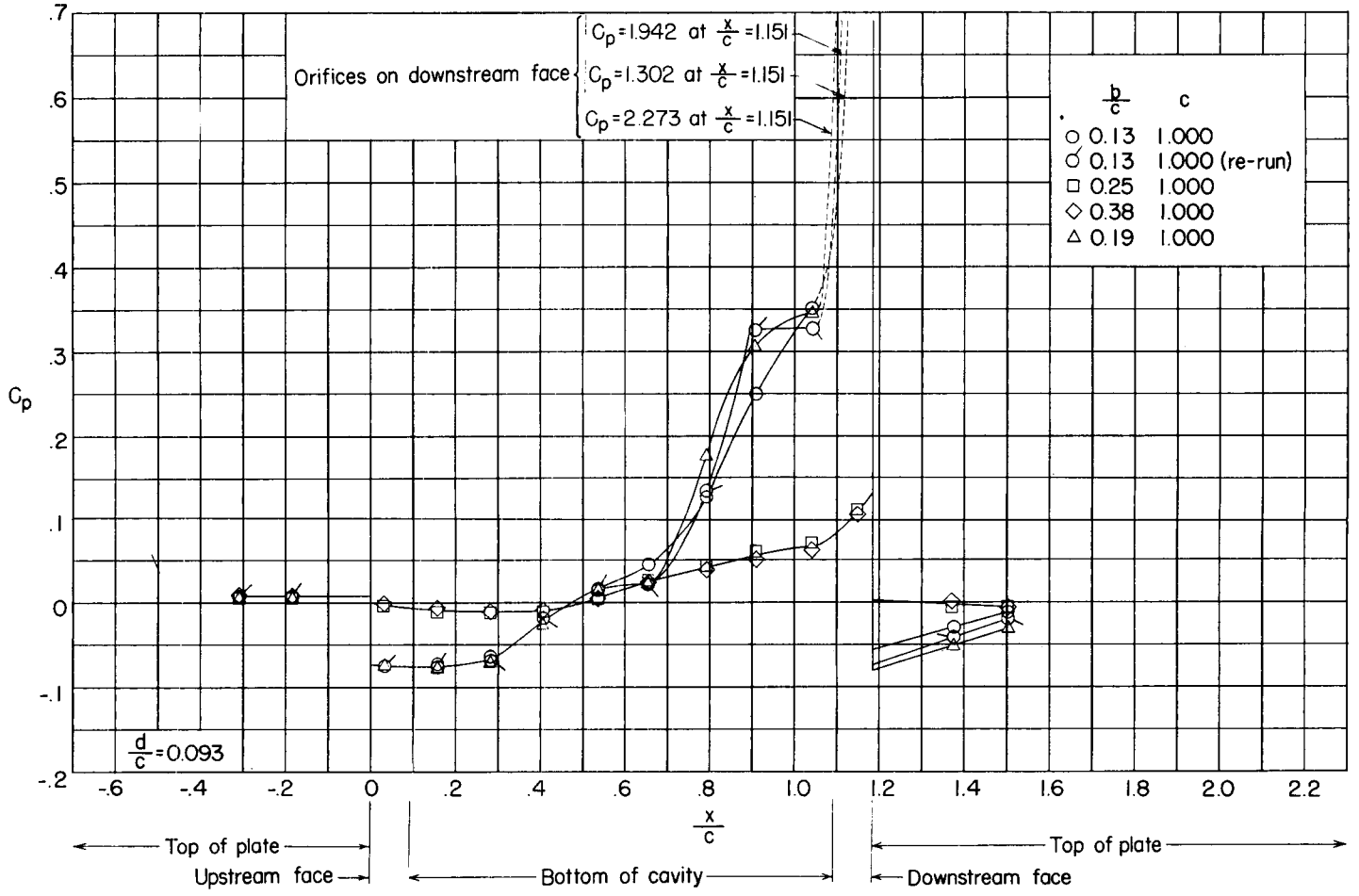

(a) Continued.

Figure 6.- Continued.

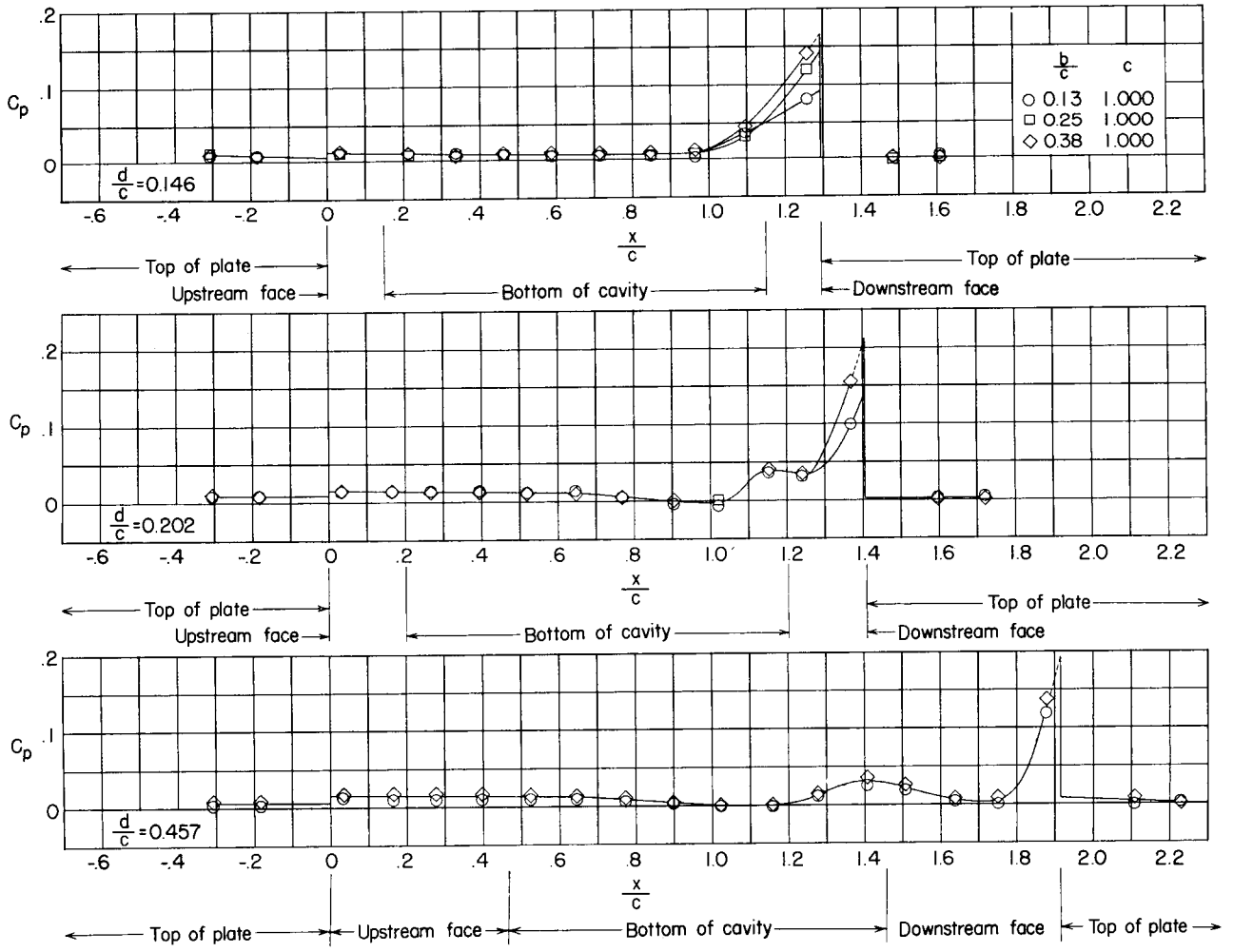

(a) Concluded.

Figure 6.- Continued.

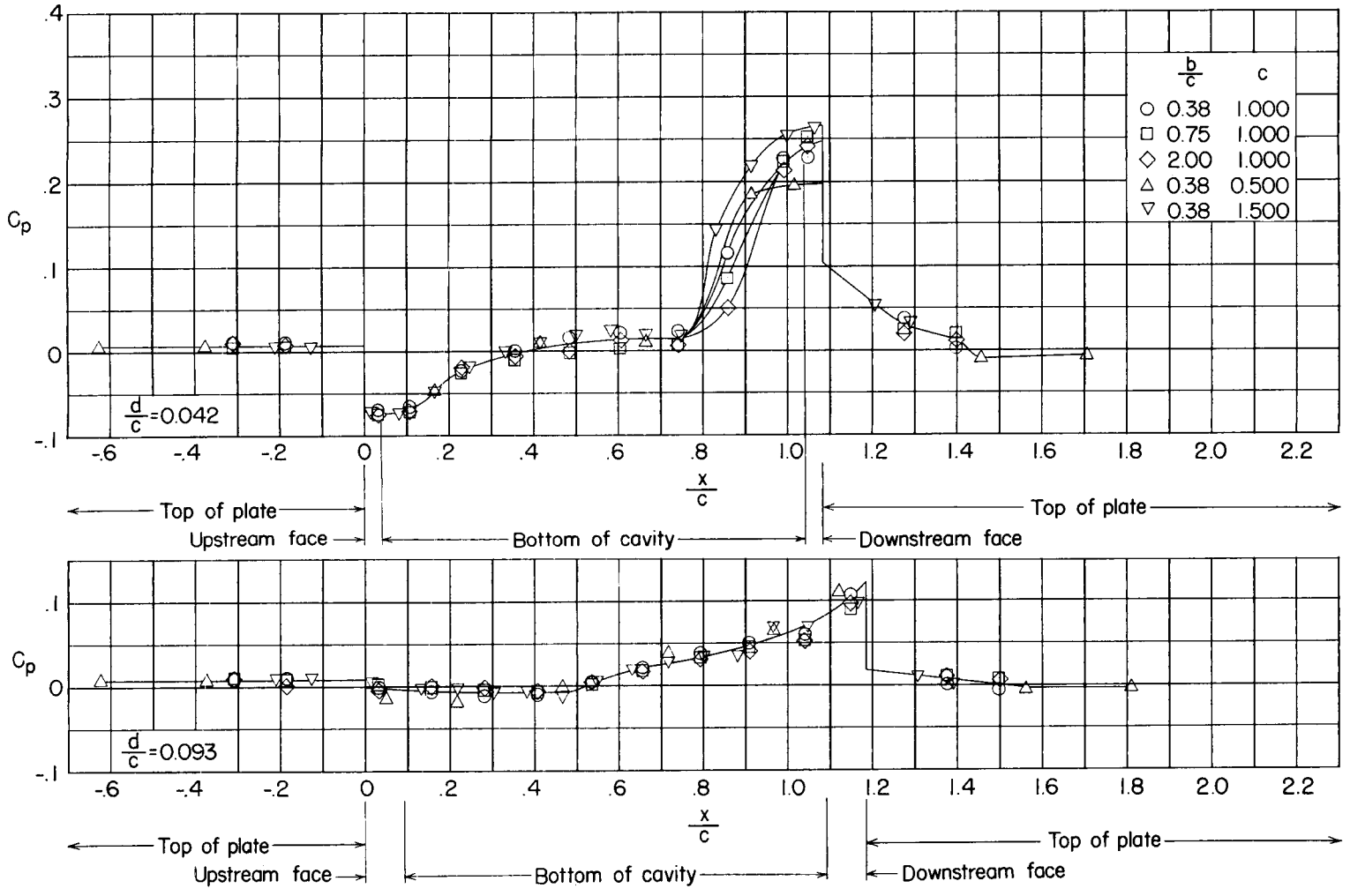

(b) $\frac{b}{c}$ = 0.38 to 2.00.

Figure 6.- Continued.

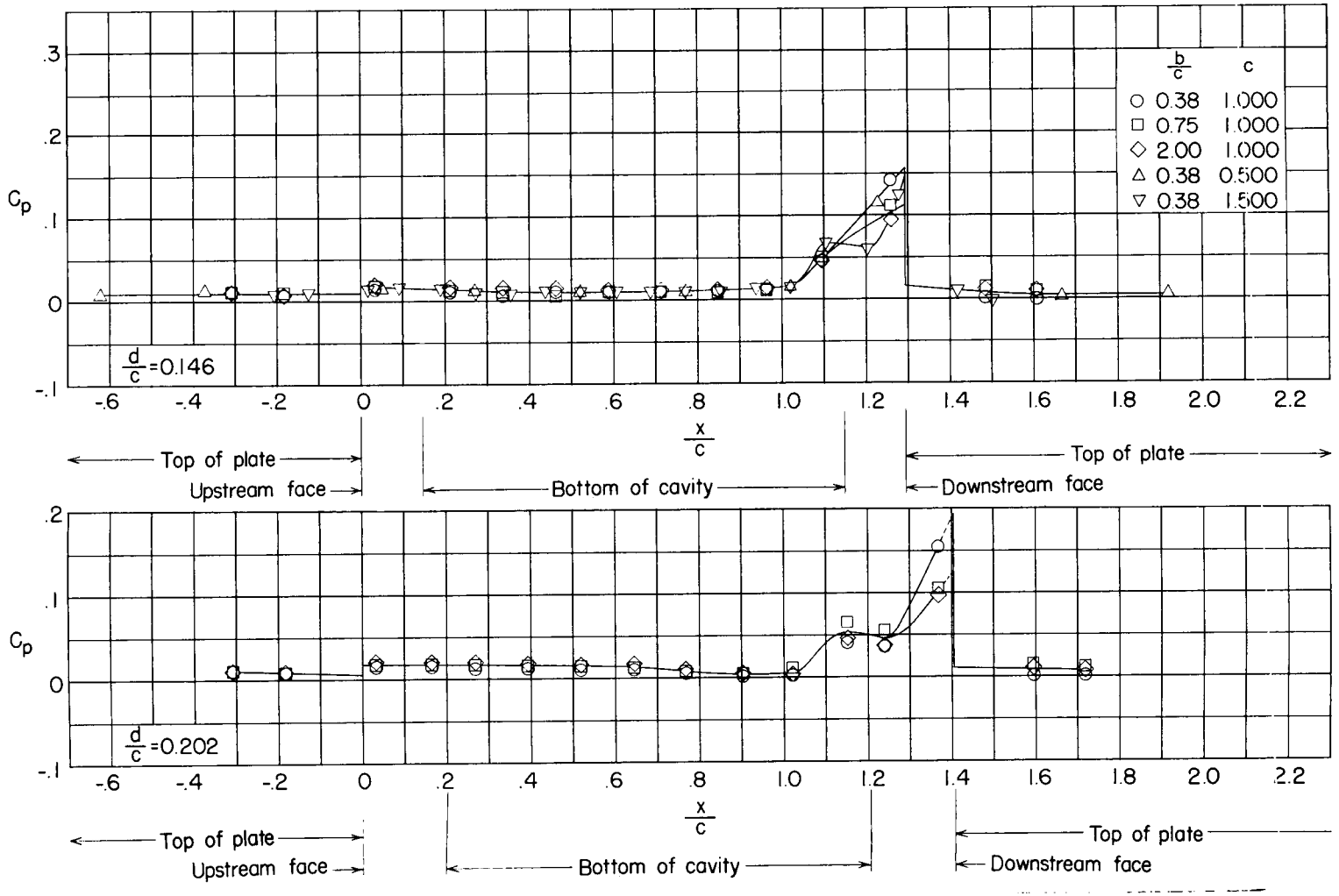

(b) Continued.

Figure 6.- Continued.

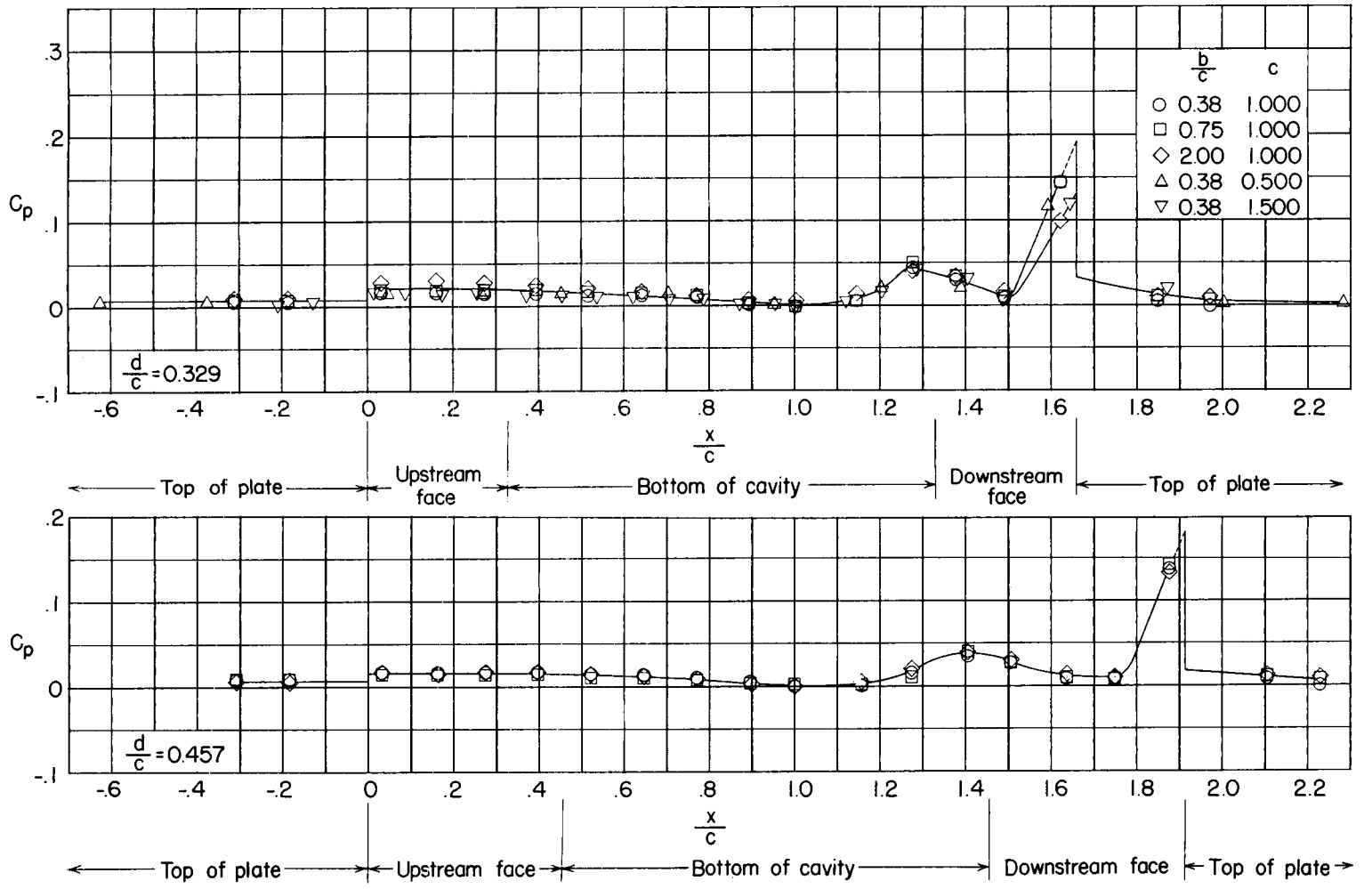

(b) Concluded.

Figure 6.- Concluded.

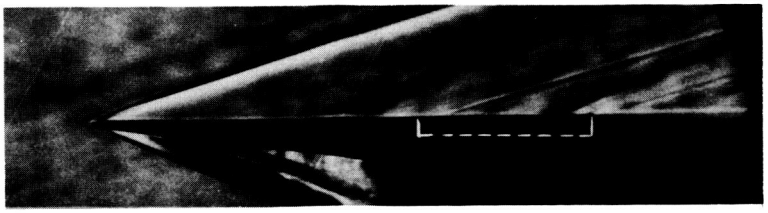

$\frac{b}{c}$=0.13, t.s. off

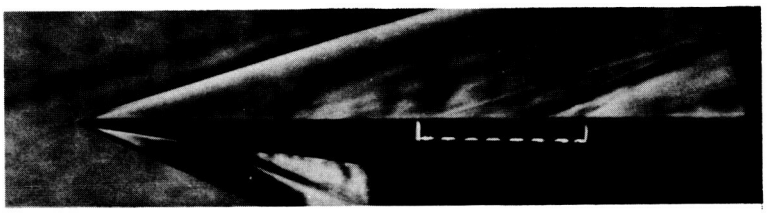

$\frac{b}{c}$=0.19, t.s. off

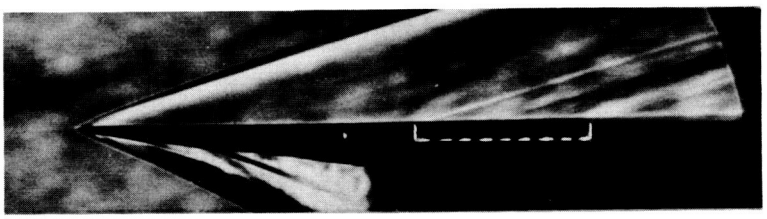

$\frac{b}{c}$=0.25, t.s. off

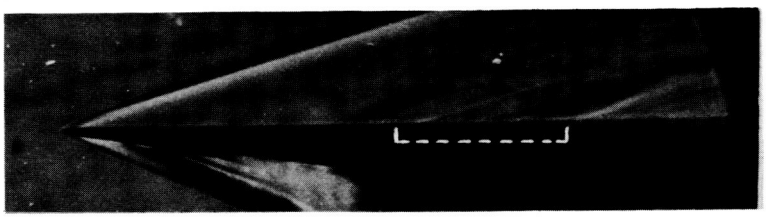

$\frac{b}{c}$=0.38, t.s. off

L-60-269

Figure 7.- Schlieren photographs showing the effects of span on the shock structure immediately above the moderately shallow cavity (d/c = 0.093). c = 1.000 inch.

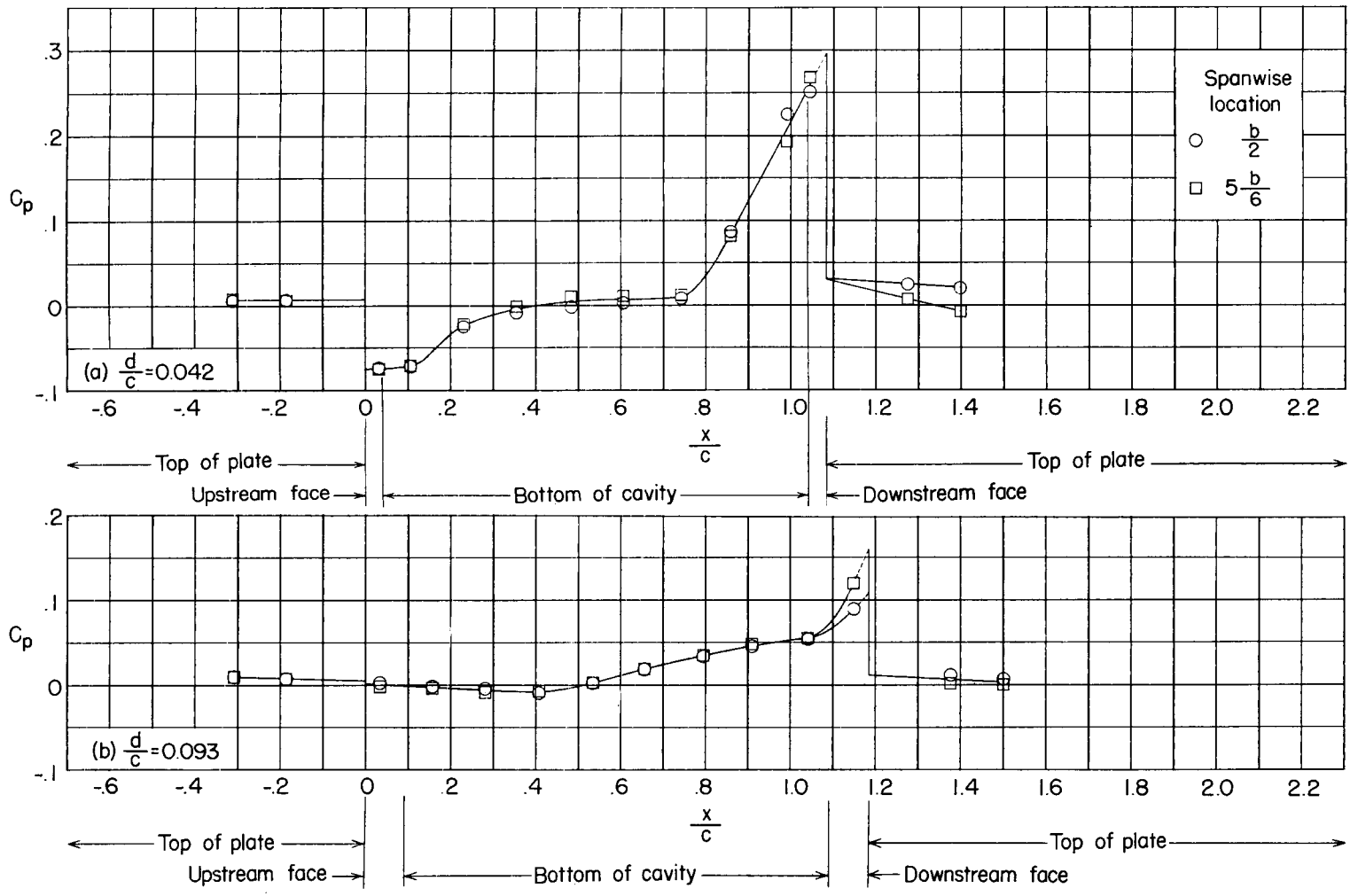

Figure 8.- Effect of spanwise location on the pressure distribution in the cavity. c = 1.000 inch; $\frac{b}{c}$ = 0.75.

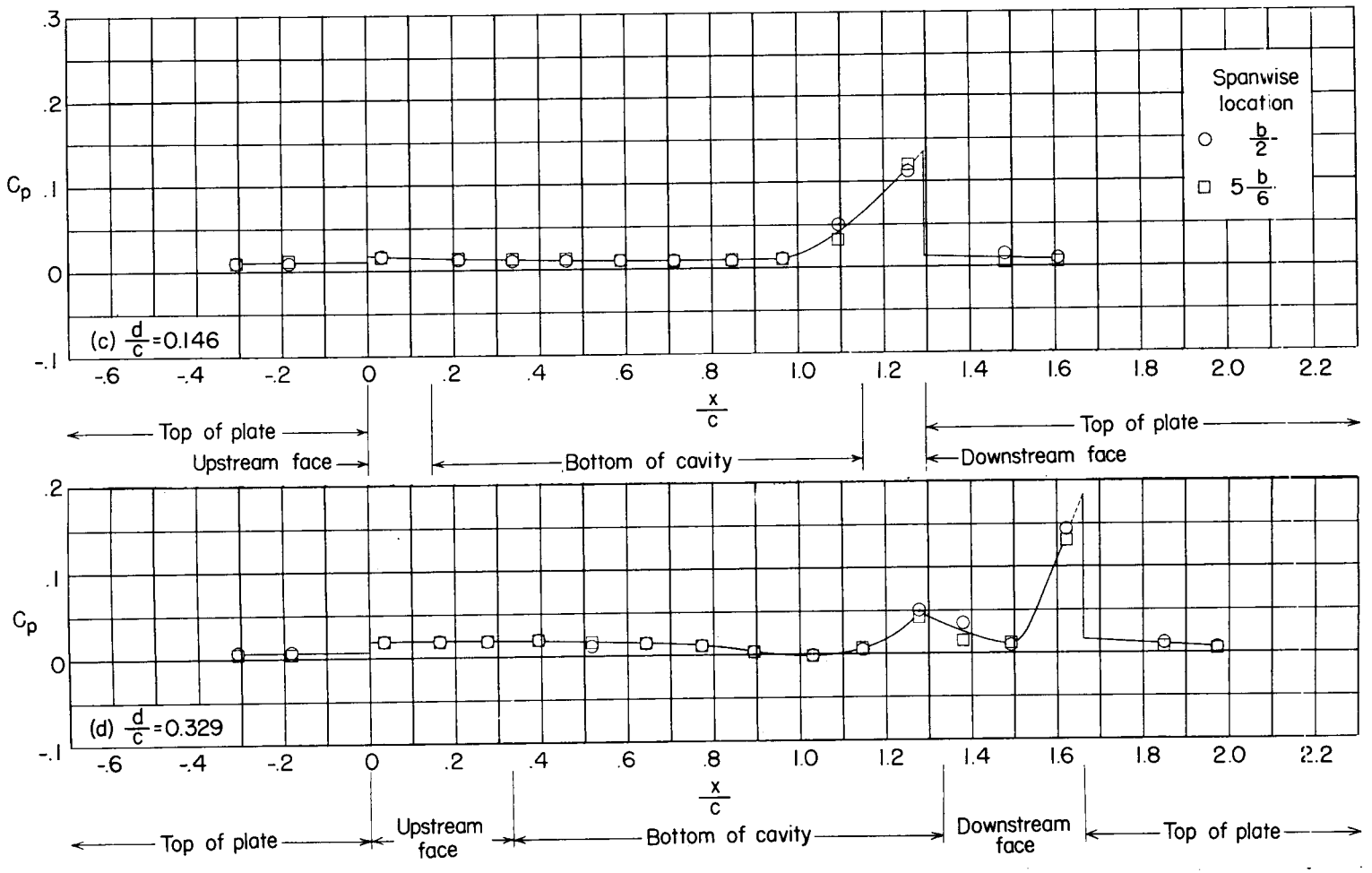

Figure 8.- Concluded.

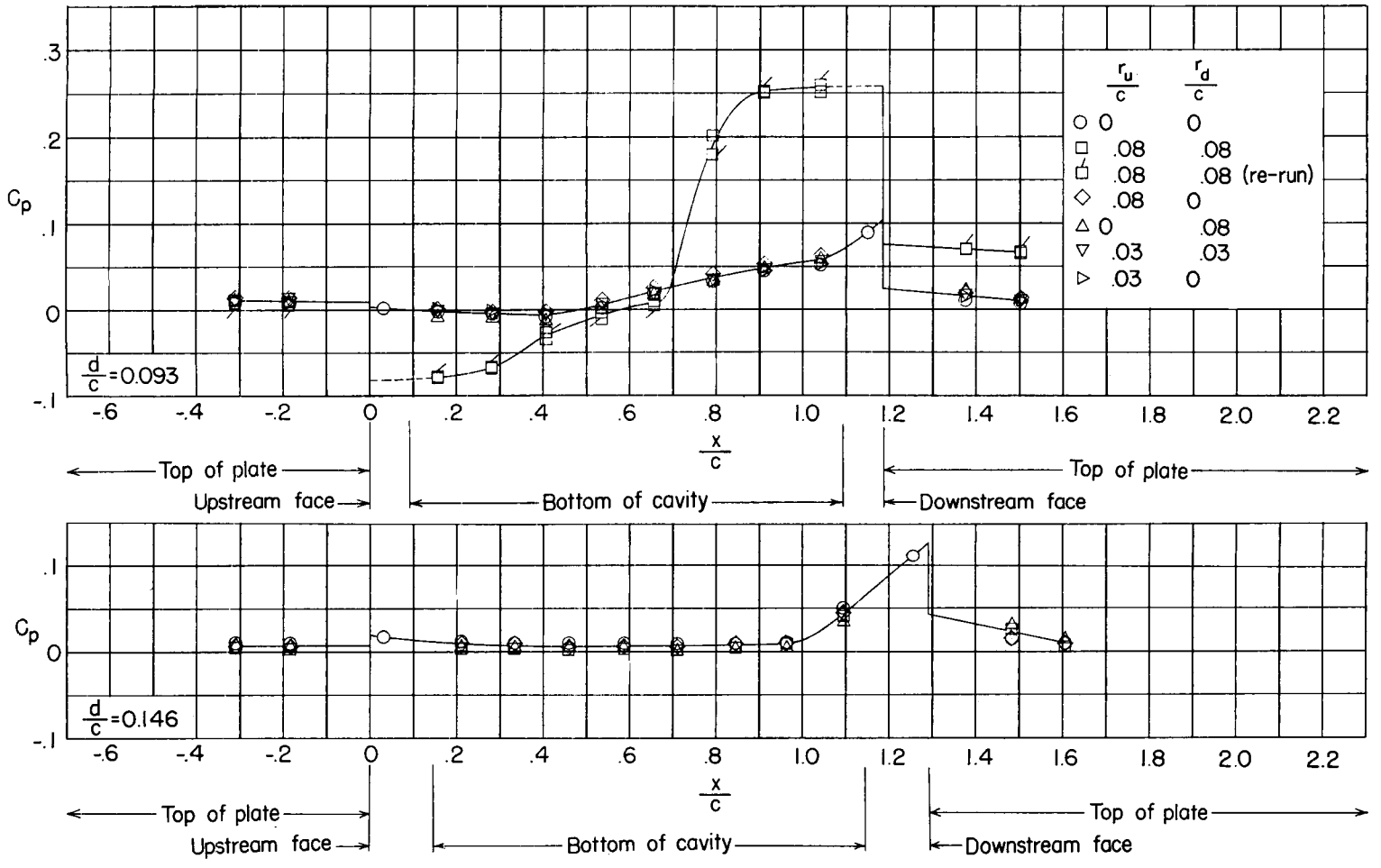

(a) $\frac{b}{c}$ = 0.75.

Figure 9.- Effect of upstream and downstream lip radii on the pressure distribution in the cavity. c = 1.000 inch. (Dashed portions of curves indicate uncertain fairing.)

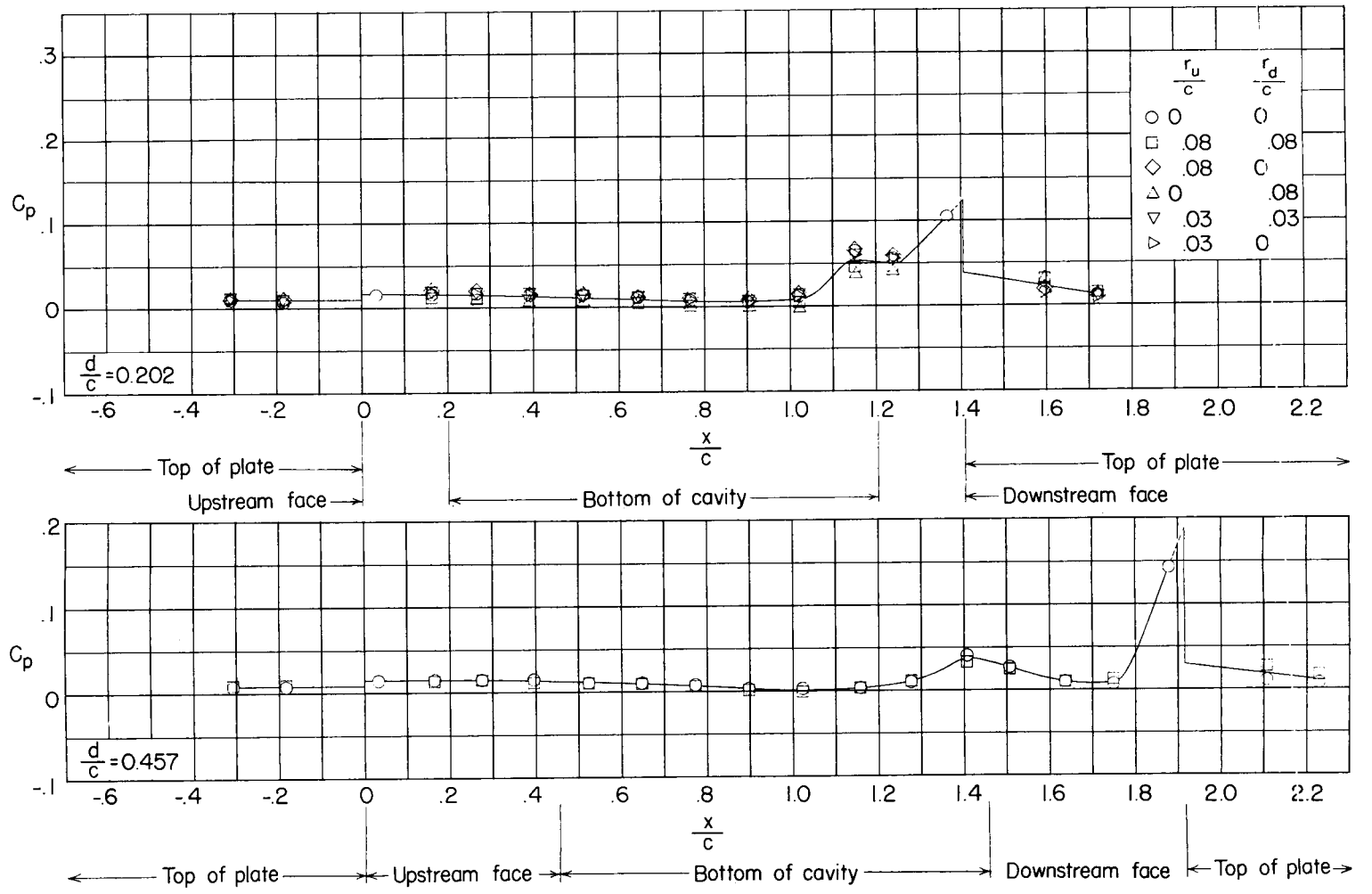

(a) Concluded.

Figure 9.- Continued.

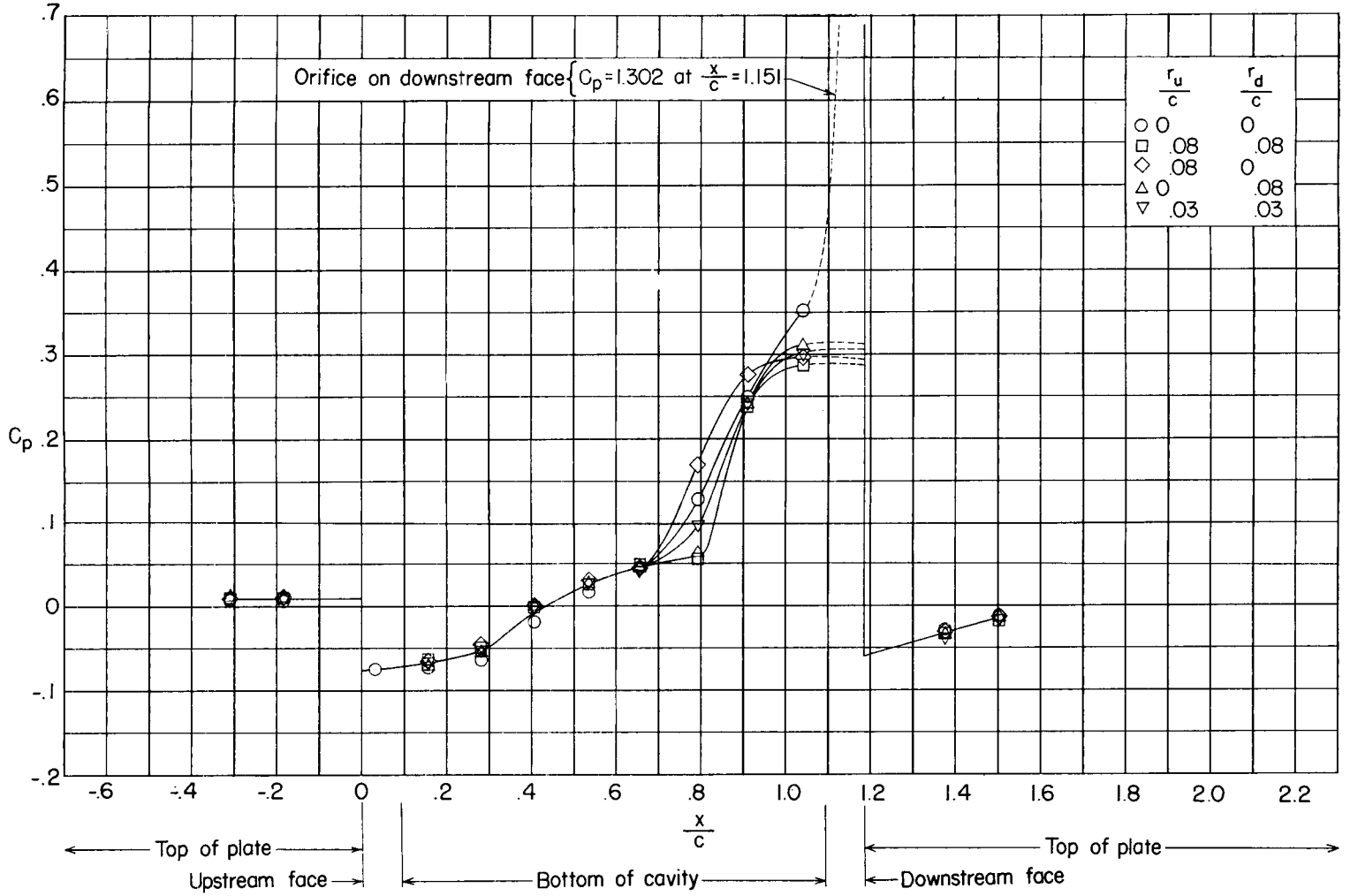

(b) $\frac{b}{c} = 0.13$; $\frac{d}{c} = 0.093$.

Figure 9.- Continued.

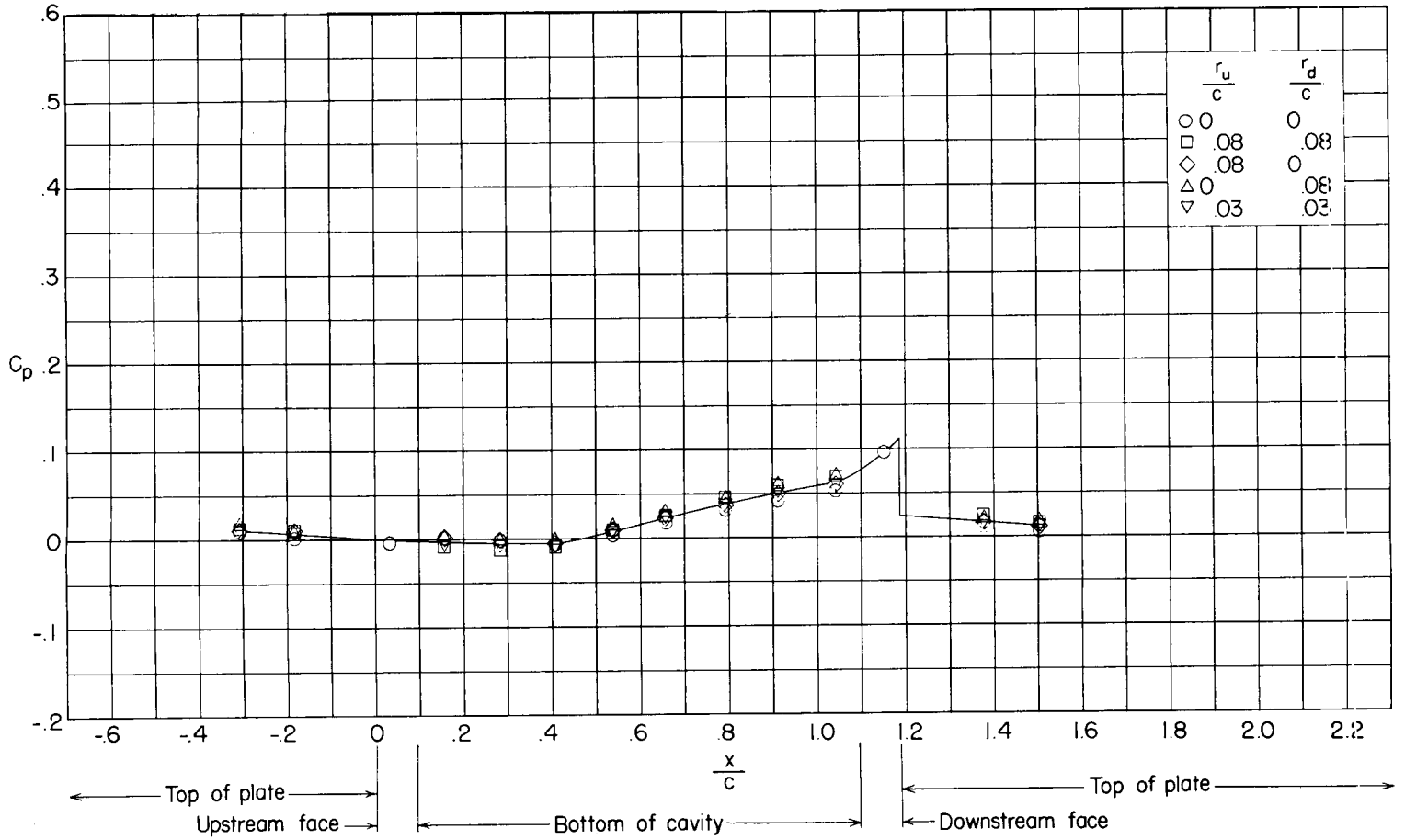

(c) $\frac{b}{c} = 2.00$; $\frac{d}{c} = 0.093$.

Figure 9.- Concluded.

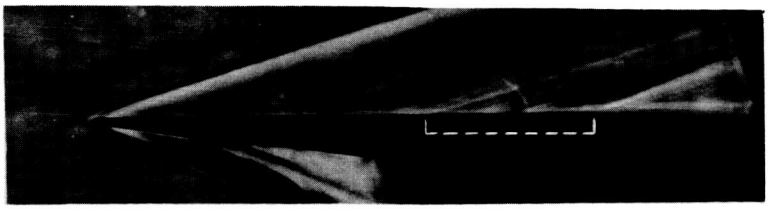

$\frac{r_u}{c}=0$, $\frac{r_d}{c}=0$, t.s. off

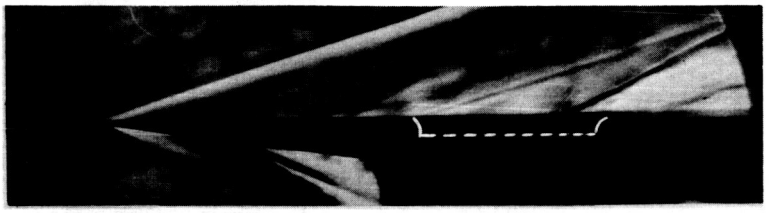

$\frac{r_u}{c}=0.08$, $\frac{r_d}{c}=0.08$, t.s. off

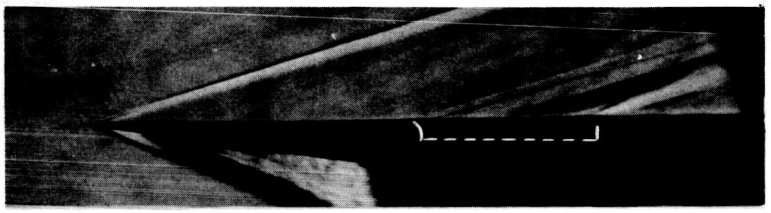

$\frac{r_u}{c}=0.08$, $\frac{r_d}{c}=0$, t.s. off

$\frac{r_u}{c}=0$, $\frac{r_d}{c}=0.08$, t.s. on

L-60-270

Figure 10.- Schlieren photographs showing the effects of upstream and downstream lip radii on the shock structure immediately above the moderately wide (b/c = 0.75), moderately shallow cavity (d/c = 0.093). c = 1.000 inch.

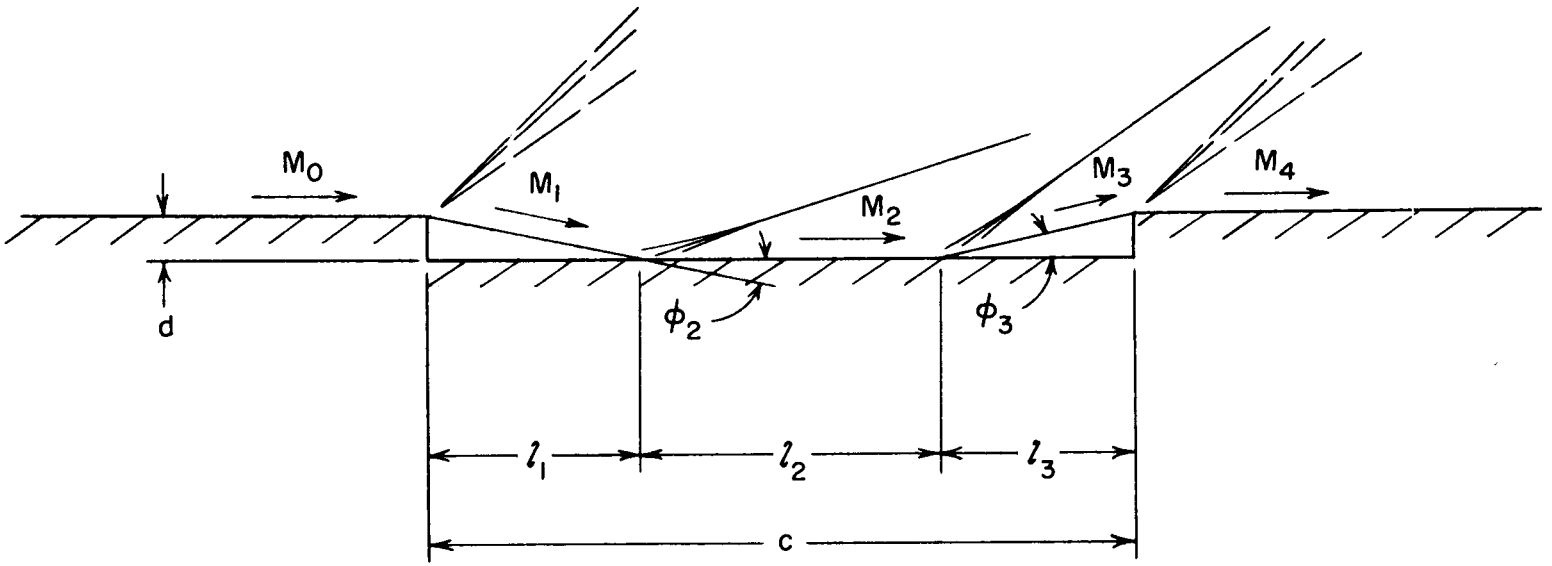

Figure 11.- Simplified version of supersonic flow in a very shallow two-dimensional cavity. $\left(\frac{d}{c} < \left(\frac{d}{c}\right)_{detached}\right)$.

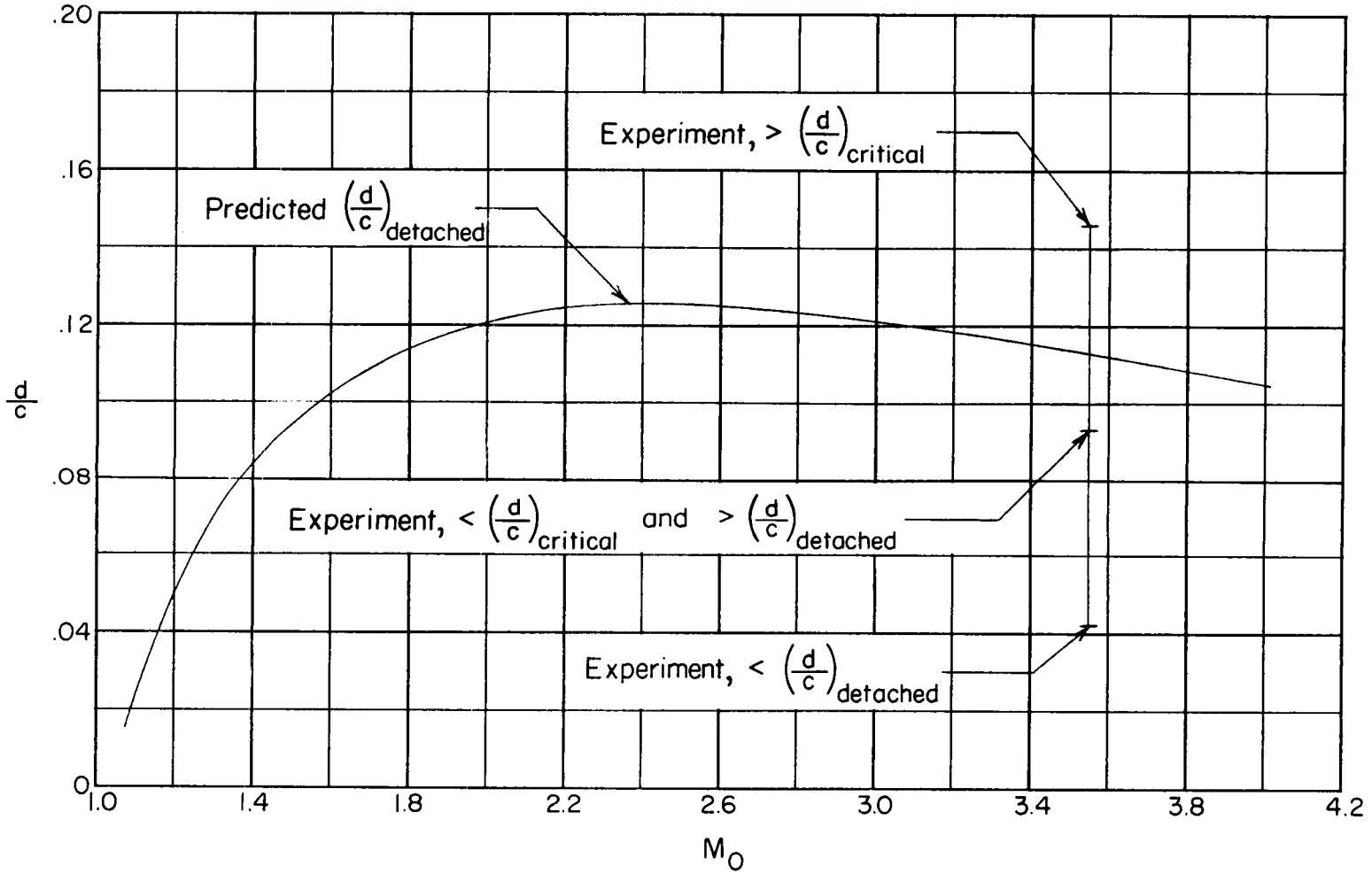

Figure 12.- Prediction of detachment depth of cavity over the supersonic Mach number range and comparison with experiment at $M_0 = 3.55$.

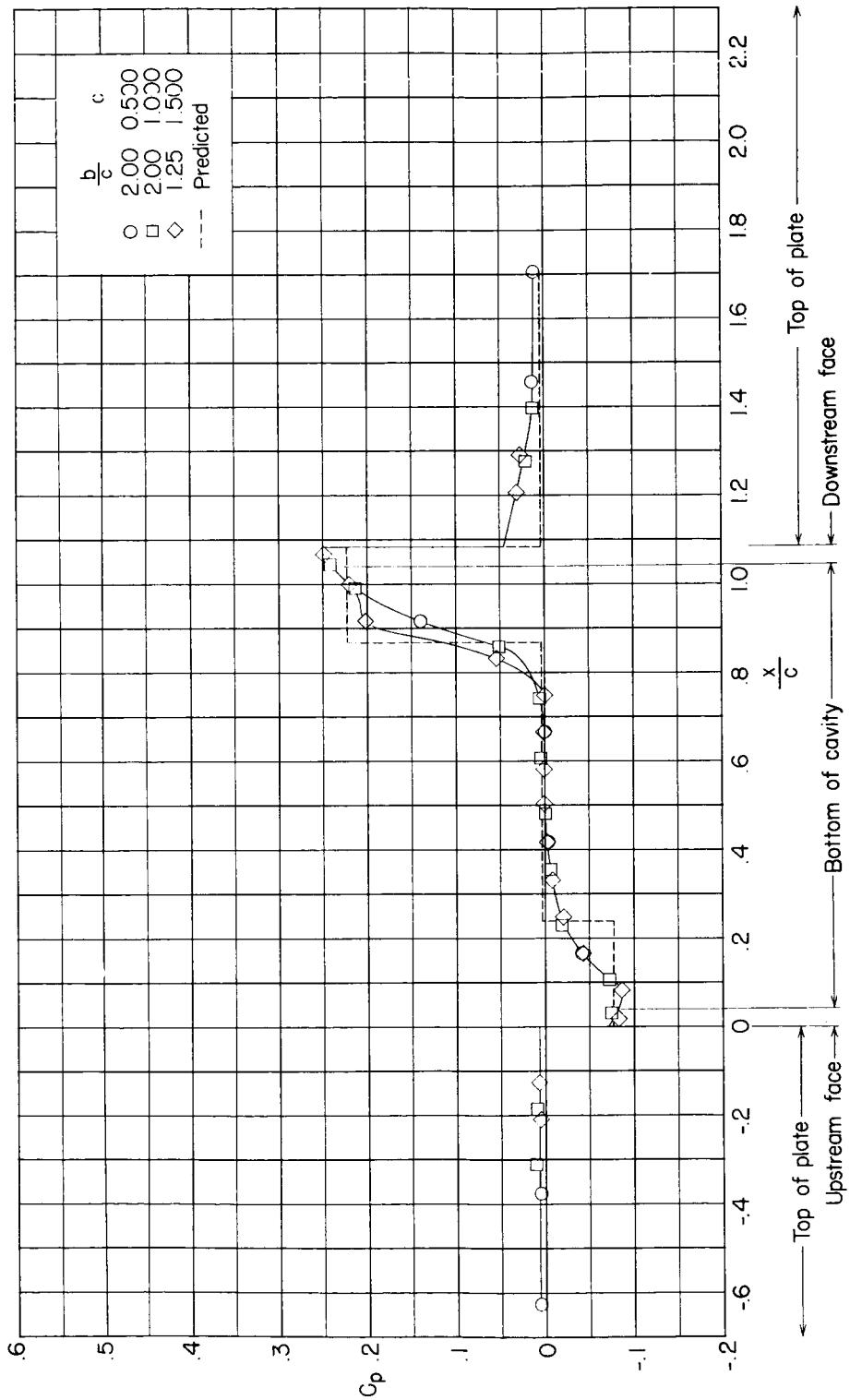

Figure 13.- Comparison of experimental pressure distribution in very shallow cavity (d/c = 0.042) with predicted pressure distribution.

L-518